Review

Patterning self-assembled monolayers

Rachel K. Smith, Penelope A. Lewis, Paul S. Weiss [*]

Departments of Chemistry and Physics, 152 Davey Laboratory, The Pennsylvania State University, University Park, PA 16802-6300, USA

Abstract

The understandings and applications of self-assembly have evolved significantly since the adsorption of *n*-alkyldisulfides on gold surfaces was first reported. The desire to produce features on surfaces that are placed in controlled proximity has driven study in both the chemistries and methodologies of their production. Self-assembled monolayers (SAMs) are found in applications such as molecular and biomolecular recognition, lithography resists, sensing and electrode modification, corrosion prevention, and other areas where tailoring the physicochemical properties of an interface is required. Patterned SAMs, in which specific self-assembling components have a deliberate spatial distribution on the surface (planar or otherwise), are generated to fabricate sophisticated nanoscale architectures and to provide well-characterized supports for physicochemical and biochemical processes. It is possible to introduce patterned features into both SAMs and the substrates that support them as the parameters controlling SAM formation and dynamics are better understood. As these structures are not at equilibrium once formed, one can manipulate the monolayer both during and after its formation by means of thermal, chemical, and electrochemical processing, exposure to controlled energetic beams, and scanning probe microscopes.
© 2003 Elsevier Ltd. All rights reserved.

[*] Corresponding author.
E-mail address: stm@psu.edu (P.S. Weiss).
URL: http://stm1.chem.psu.edu

Contents

1. Introduction

The interactions between molecules and surfaces are some of the most exciting and widely studied aspects of modern surface science. The strengths of the interactions between molecules and substrates are highly dependent upon their chemical natures, ranging from very weak (e.g., *n*-alkanes adsorbed on gold or graphite [1]) to strong enough to break chemical bonds within the molecule (e.g., ethylene on platinum [2]). One of the most remarkable molecule–substrate interactions is the spontaneous self-organization of atoms and molecules on surfaces into well-ordered arrays; the supramolecular assemblies that form often possess both short- and long-range order. In particular, the spontaneous organization (self-assembly) of surfactant molecules adsorbed on transition metal surfaces has been of growing importance over the past two decades. The field of self-assembly has grown rapidly since the discovery of these structures and their ability to modify the physical and chemical properties of a surface, Fig. 1 [3–5]. Studies of these thin films have ranged from the very basic (studying the fundamental organizations and chemistries of the systems) to the applied (examining the robustness and chemical utilities of these assemblies once formed and placed in desired environments).
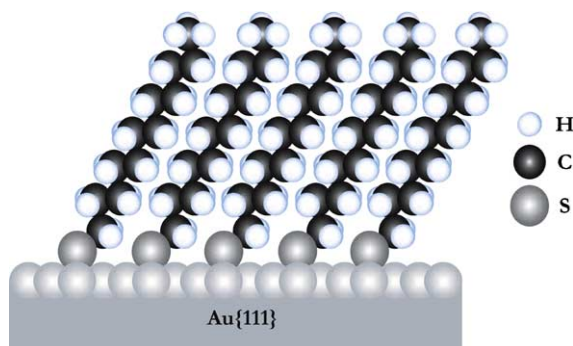
Fig. 1. Schematic of an *n*-dodecanethiolate monolayer self-assembled on an atomically flat gold substrate. The assembly is held together by the bonds between the sulfur headgroups and the gold surface as well as van der Waals interactions between neighboring hydrocarbon chains.

Acronyms

2,4-DNP 2,4-dinitrophenol
3-MPA   3-mercaptopropionic acid
AFM   atomic force microscopy (microscope)
BSA   bovine serum albumin
CAD   computer-assisted design
CAG   contact angle goniometry
CS-AFM current sensing atomic force microscopy (microscope)
DPN   dip-pen nanolithography
EBE   electrochemical blocking effect
ECR-RIE electron cyclotron resonance-reactive ion etching
ESCA   electron spectroscopy for chemical analysis
Fc   ferrocene
FT-IR   Fourier transform infrared spectroscopy
IgG   Immunoglobulin G
L–B   Langmuir–Blodgett
LFM   lateral force microscopy (microscope)
MHDA   16-mercaptohexadecanoic acid
MIMIC   micromolding in capillaries
NEXAFS near edge X-ray absorption fine structure
NSOM   near-field scanning optical microscope
nTP   nanotransfer printing
ODT   *n*-octadecanethiol
oEG   oligo(ethylene glycol)
OPE   oligo(phenylene–ethynylene)
OTS   octadecyltrichlorosilane
PDMS   polydimethylsiloxane
PS   polystyrene
QCM   quartz crystal microgravimetry
RGD   arginine–glycine–asparagine
RM   replica molding
SAM   self-assembled monolayer(s)
SAMIM   solvent-assisted micromolding
SECM   scanning electrochemical microscopy (microscope)
SEM   scanning electron microscopy
SPL   scanning probe lithography
SPR   surface plasmon resonance
STM   scanning tunneling microscopy (microscope)
TODE   topographically-directed etching
TPD   thermal programmed desorption
μCP   microcontact printing
UDT   *n*-undecanethiol

UHV	ultra-high vacuum
μTM	microtransfer molding
UV	ultra-violet
XPS	X-ray photoelectron spectroscopy

The concept of molecules organized into higher order structures is not new [6]. Examples of the ordering of atoms and molecules have been shown throughout biology, chemistry, and physics. In the context of surface chemistry, however, it is important to mention that amphiphilic molecules spontaneously organizing into assemblies on metal surfaces are only a subset of self-assembled films that have been reported and characterized. Molecules that are amphiphilic can organize themselves at a variety of interfaces (liquid–liquid, air–liquid, solid–liquid, and solid–air interfaces); of particular relevance to this type of surface chemistry are Langmuir–Blodgett (L–B) films, in which amphiphilic molecules organize at one interface (typically air–solution) and are transferred to another (air–solid). However, L–B films are known to suffer both in chemical and mechanical stabilities and will not be covered in the scope of this review; therefore the trend of research has pointed to the creation of the more environmentally and chemically stable systems of assemblies chemically bound to solid surfaces. These systems can possess order at the nanometer scale, as well as higher degrees of order imposed upon their assembled structure and will be a focus of this review.

Many different chemistries for the adsorption of amphiphiles on surfaces have been studied over the past twenty years, encompassing a range of substrates and a greater variety of adsorbates. Self-assembled monolayers (SAMs) are typically formed from the exposure of a surface to molecules with chemical groups that possess strong affinities for the substrate or a material patterned on it. How well these assemblies order is a function of the nature of the chemical interaction between substrate and adsorbate, as well as the type and strengths of intermolecular interactions between the adsorbates that are necessary to hold the assembly together. Molecules "binding to" surfaces are either described in terms of physisorption, in which the enthalpies of interactions are rather low (considered to be $\Delta H < 10$ kcal/mol, typically from van der Waals forces), or in terms of chemisorption with $\Delta H > 10$ kcal/mol. Strengthening interactions between molecules and substrates and between molecules themselves include phenomena such as hydrogen bonding, donor–acceptor and/or ion pairing, and the formation of covalent bonds, rendering the assemblies more stable than their physisorbed counterparts. Other studies have focused upon directly "grafting" molecules to surfaces, such as the attachment of aryl-functionalized molecules to silicon [7], alkyl-functionalized molecules to germanium via Grignard reactions [8], and molecules to metal surfaces through diazonium salts [9,10], all of which indicate the formation of surface–carbon bonds.

Chemisorbing systems have included the assembly of trialkyl-, trichloro-, or trialkoxysilanes on silicon dioxide surfaces [5,11–13], carboxylic acids adsorbing onto
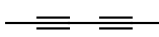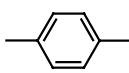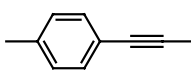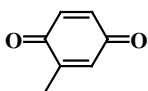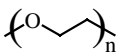
aluminum oxide and silver surfaces [14–16], and *n*-alkanethiols chemisorbing to gold surfaces [3,17,18], to name merely a few. As noted above, particularly well-studied SAMs are those formed on transition metal surfaces (e.g., Au, Ag) and surfactants with electron-rich headgroups (e.g., S, O, N) and *n*-alkyl tails. The affinities between the surfaces and headgroups are strong enough to form either polar covalent or ionic bonds, and favorable lateral interactions between adjacent molecules are sufficient to draw and to hold the assembly together. A schematic of a SAM of *n*-alkanethiolate molecules chemisorbed to a gold surface is shown in Fig. 1.

When the first reports of self-assembled thin films emerged in the literature, the chemical character of the molecules used included a polar headgroup such as a thiol or carboxylic acid as well as a simple, hydrophobic overlayer (generally linear and aliphatic). Today, the molecules used can possess a number of functional groups in addition to the moiety responsible for the molecule's chemisorption. These functional groups can be buried near the film–substrate interface, distributed within the film interior, and/or located at the terminus of the molecule that presents itself to the film–air interface (Table 1). Variation in the chemical contact between the molecule and the metal substrate controls the strength of the interactions (and thus stability) of the assembly and also how easily electrons are transmitted from the molecule to the metal under an applied potential [19–21]; manipulation of the film interior affects its innate ability to order or affects how easily electrons are conducted through the film [22–26]. The terminal functional group of a SAM is critical to its interfacial properties—the surface's general hydrophobic/hydrophilic character, adhesive characteristics, and reactivity; especially noteworthy is the ability to perform chemical reactions using the pendant functional groups (i.e., carboxylic acids, quinones, amines, anhydrides). Meanwhile, the nature of the lateral interactions holding together the supramolecular assembly has varied, now expanding from the all-*trans* (fully extended, minimal disorder) aliphatic chains that were reported in initial studies. In fact, several examples of well ordered SAMs have been reported from linear phenylene [27–29], phenylene–ethynylene [26], and phenylene–vinylene fragments [25] with sulfur headgroups. Both covalent and non-covalent interactions between adsorbates have assisted in producing well ordered SAMs, such as those with crosslinked interiors [30–33] or by the addition of hydrogen bonding groups to impart stability [34–36]. SAMs can also have terminal groups with switchable conformations, such as those terminated with oligo(ethylene glycol) (oEG) groups;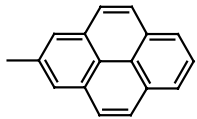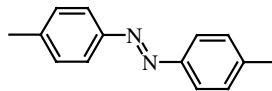 electric fields on the order of 1 V/Å can cause coiling of the terminal methoxy groups, which may ultimately affect the assembly's ability to resist protein adsorption [37–39]. Although the structural elements within the SAM can vary, the important factor for its stability is the strength of the attractive interactions between neighboring molecules.

SAMs are of prime technological interest, as the presence of molecules chemically bound to the surface renders the properties of the modified interface (i.e., wetting, conductivity, adhesion, and chemistry) to be entirely different than those of the bare substrate. The exposed terminal functional group(s) of the SAM can be further modified so as to enhance or to alter the film properties. Changing the groups exposed at the air–film surface is critical for determining and designing the interaction

Table 1
Various functional groups that have been incorporated into thiol-based SAMs, whether within the interior (I) of the film or at the terminus (T). Substituents have been omitted for clarity, and sites of attachment to the remainder(s) of the thiol-based molecule are indicated by a '–' off of the listed moiety

Functional group	Name	I	T	Selected reference(s)
$-CH_3$, $-CH_2-$	Alkyl	✔	✔	[17,40,41]
$-CF_3$, $-CF_2-$	Trifluoromethyl, difluoromethylene	✔	✔	[42,43]
$-CH_2OH$, $-CH_2OCH_2-$	Hydroxyl, ether	✔	✔	[40,41,44–49]
$-COOH$, $-COO^-$	Carboxylic acid		✔	[40,50,51]
$-CO_2CH_3$, $-CO_2CH_2-$	Ester	✔	✔	[52]
$-CONH_2$, $-CONH-$	Amide	✔	✔	[34,35,53,54]
$-Cl$, $-Br$	Chloro, bromo		✔	[17,40,51]
$-CN$	Nitrile		✔	[17,51,55]
$-NH_2$, $-NH_3^+$	Amine		✔	[48,56]
$-B(OH)_2$	Borate		✔	[57]
	Alkene	✔		[17,49]
	Alkyne	✔		[49]
	Diacetylene	✔		[30,31,33,58,59]
	Aryl	✔	✔	[27,60]
	Oligo(phenylene–ethynylene), OPE	✔		[29,61–64]
	Quinone		✔	[65]
	Oligo(ethylene glycol), oEG		✔	[38,66–68]
	Sulfone	✔		[69]
	Epoxide		✔	[70]
	Pyrene		✔	[71,72]
	Azobenzene	✔		[61,73,74]

strengths of proximal molecules or analytes (i.e., sensing, electron transfer, cell adhesion, polymer adsorption) or for post-assembly modification of the film. Molecules that are confined to the air–film interface can undergo selective chemistry, as they are confined to two dimensions; unlike (three-dimensional) solution-phase chemistry, the molecules are held in fixed conformations. The incorporation of functional moieties such as chromophores, electroactive groups, or molecules that can bond within the SAM (i.e., covalent cross-linking between adjacent molecules or non-covalent hydrogen bonding) enable capabilities in sensing, electron transfer, molecular recognition, and other areas. Many technologically relevant materials possess well-defined surface chemistries, including metals, semiconductors, oxides, and other complex materials such as superconductors; a variety of heteroatom-containing molecules have been shown to self-assemble on such substrates (Table 2). The nature of interactions between molecules and substrates range from hard acid–base interactions to soft donor–acceptor charge transfer interactions. However, there are a number of materials that possess complex and varied surface chemistries. Complex materials (e.g., some oxides, ferroelectric materials such as $LiNbO_3$ and others) possess crystal structures with a number of atomic constituents; often times, their surfaces are enriched in a particular element due to processing and the chemical environment (e.g., exposure of lead zirconate titanate ($PbZrTiO_3$) to acidic conditions leads to a surface that is lead-depleted). Certain areas of a material can be selectively protected so as to create a distribution of chemical compositions within the same material, or for the purpose of further growth or etching.

   The physical and chemical properties of SAMs (*vide infra*) leave them amenable to further manipulation, thus creating *patterns* within the film. Within the following

Table 2
Chemical systems of adsorbates and substrates that form SAMs

Surface	Substrate	Adsorbate(s)	Selected reference(s)
Metal	Au	R–SH, R–SS–R, R–S–R, R–NH$_2$, R–NC, R–Se, R–Te	[17,75–78]
	Ag	R–COOH, R–SH	[18,79]
	Pt	R–NC, R–SH	[80–82]
	Pd	R–SH	[83]
	Cu	R–SH	[84]
	Hg	R–SH	[85]
Semiconductor	GaAs (III–V)	R–SH	[86,87]
	InP (III–V)	R–SH	[88]
	CdSe (II–VI)	R–SH	[89]
	ZnSe (II–VI)	R–SH	[90]
Oxide	Al$_2$O$_3$	R–COOH	[14]
	TiO$_2$	R–COOH, R–PO$_3$H	[91,92]
	YBa$_2$Cu$_3$O$_{7-\delta}$	R–NH$_2$	[93,94]
	Tl–Ba–Ca–Cu–O	R–SH	[95]
	ITO	R–COOH, R–SH, R–Si$(x)_3$	[96,97]
	SiO$_2$	R–Si$(x)_3$	[5]

sections, we will discuss the nature of SAMs, techniques employed to study their formation and structures, describe how they have been patterned, and how their formation has been of utility for applications as lithography resists, as supports for cell growth and adhesion, in electrochemistry, and more. As SAMs are of such exceptional technological importance, there is a great desire to control their features, or the features of the substrates supporting them, down to the nanometer scale as technology continues to shrink in size and dimension. Self-assembly has been a useful method with which to isolate and to study molecules and assemblies at the nanoscale. The invention and development of scanning probe microscopes (*vide infra*) have greatly enhanced our ability to understand and to optimize the patterning of SAMs, as the spatial distributions of individual adsorbates can be directly measured.

2. Patterning self-assembled monolayers

As we have gained understanding and control of SAMs, it has only been natural to increase the complexity of these thin organic films. As the mechanisms of their formation and their manipulation are increasingly understood, SAMs have been prepared with both single and multiple components in predetermined spatial distributions; more simply, SAMs have begun to be patterned. This patterning has been engineered in a variety of ways, either by the selective *removal* of particular adsorbates, by the selective *placement* of adsorbates, by the selective *reaction* of adsorbates, by their destruction with energetic beams, or by their deliberate removal with scanning probe microscopes moving in a determined rastering pattern and the application of force or delivery of low energy beams, Fig. 2 and Table 3. Once adsorbates have been placed on the surface at sub-monolayer coverage, the remaining surface area can be left bare or the exposed regions of surface can be "backfilled" with a new adsorbate.

Not only has there been intense interest in manipulation of the SAMs themselves in order to create complex thin films, SAMs are also used as ultra-thin organic resists in lithography. As a protective organic layer has been shown to reduce the etching of metal surfaces drastically when exposed to oxidizing solutions, features can be patterned into the substrate that support the SAM since the etch rates differ between bare metal and the SAM-covered metal [98–105]. Therefore, SAMs have been used as *sacrificial* structures to create patterns into metal with a resolution that is often either difficult, time-consuming, or expensive to achieve with state-of-the-art, conventional lithographic tools. Efforts have also been made to produce sub-micron-scale patterns on curved substrates, such as lenses, capillaries, and fibers [106], enabling the microfabrication of devices in increasingly confined spaces.

It is important to pattern films in order to understand the fundamental interactions and organization of mixed monolayers on surfaces, but an additional reason for patterning SAMs is to create functional nanostructures completely or in part from the "bottom up". Using particular chemical functional groups or using mixed-component SAMs, features of interest such as nanoparticles, cells, proteins, or other
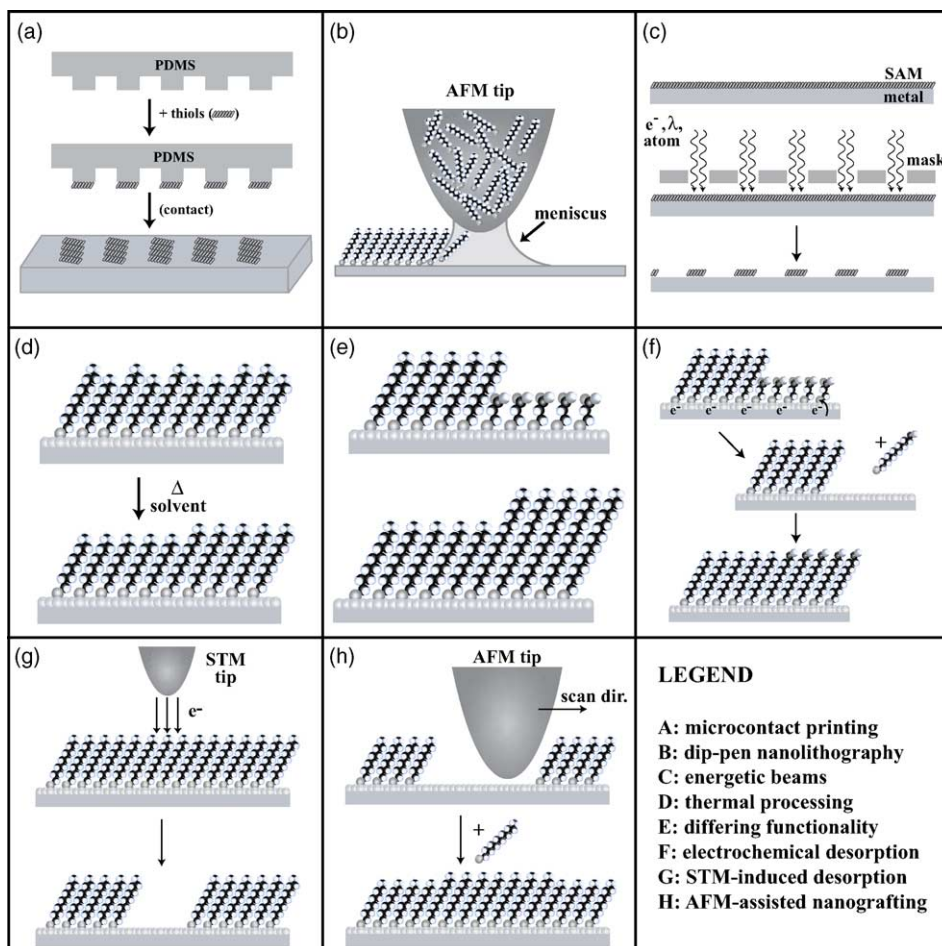
Fig. 2. Schematics of several techniques employed to pattern SAMs (see text for discussion).

biomolecules can be patterned for the creation of higher-ordered structures and architectures if they possess particular affinities for parts of the SAM. The development of patterned SAMs is critical as they can serve as both sacrificial structures (a means to an end), as well as both final structures or supports, as the patterning of particular molecules imparts a predisposed reactivity to a surface.

Patterned SAMs are also important in applications for nanotechnology. With the information that we and others have garnered on the molecular-scale organization of multicomponent self-assembling films, we have begun to use self-assembly as a significant experimental approach and a method to isolate and to probe molecules that are candidates for novel nanocircuit components [62,63]. One criterion for the development of nanoelectronic devices is being able to position and to pattern molecular components selectively on surfaces, thus imparting regularity to the

Table 3
Current capabilities of various SAM patterning techniques (see text for references)

Technique	Approximate resolution (nm)	Area	Comments
(A) Microcontact printing (μCP)	30	>cm^2	Fast, parallel
(B) Dip-pen nanolithography (DPN)	10	<mm^2	Slow, serial
(C) Energetic beams (e$^-$, ions, photons)	100	>cm^2	Fast, parallel
(D) Solvent/heat reorganization	100–500	>cm^2	IC
(E) Differing functionality	10–50	>μm^2	NC
(F) Electrochemical desorption	10–50	>μm^2	IC
(G) STM-assisted desorption	>1	nm^2–μm^2	Slow, serial
(H) AFM-assisted nanografting	>1	nm^2–μm^2	Slow, serial

The letter preceding the technique corresponds to its schematic in Fig. 2. Resolutions and areas are approximate. "NC" (negative control) indicates knowledge of component behavior, but ability to place molecules positively; "IC" (intermediate control) implies that when used in tandem with other techniques, greater control can be had over component placement in the SAM.

overall structure. Understanding the local intermolecular interactions of molecules on surfaces from information provided by scanning probe microscopes will permit the rational design of molecular-scale surface structures.

3. Self-assembled monolayers

3.1. The n-alkanethiolate SAM

Much research has been focused on the self-assembly of *n*-alkanethiolate and related molecules on gold substrates. Thiol-based SAMs are attractive structures for several reasons. Well-ordered SAMs can be formed from a variety of sulfur-containing species (i.e., thiols, sulfides, disulfides [3]), yet experiments show that thiol molecules kinetically outcompete the disulfide molecules for available surface sites when the two species are coadsorbed from solution [41]. The gold surface is relatively chemically inert; it does not readily form a surface oxide nor keep a strong hold of adventitiously adsorbed material, and therefore SAMs can easily be prepared in ambient conditions. SAMs render an ordinarily conductive metal surface to be relatively insulating, yet electrons can be moved controllably through the film through applied potentials when integrated into electrochemical cells (*vide infra*). Additionally, the molecules are stable once adsorbed on the surface, yet they can be affixed to the gold such that they can be selectively processed after adsorption. Many different chemical functional groups have been incorporated into *n*-alkanethiolate SAMs (Table 1). Much research has focused on the incorporation of differing terminal groups into SAMs, for interfacial properties such as hydrophobicity and reactivity to be manipulated and controlled. Recognition factors can be incorporated into the exposed interface of a SAM for either cell adhesion [68], selective protein interactions [67], or for inhibiting the non-specific binding of proteins [107]. The structures of SAMs as well as the dynamics of their formation will be discussed presently, as

alkanethiolate SAMs have often provided the foundation for increasingly complex and functional nanoscale architectures. It is through such fundamental studies of SAMs that the most efficient and effective applied systems can be created and developed.

The surface structures formed by the adsorption of *n*-alkanethiols on gold surfaces are generally well ordered and crystalline. Upon exposure of a gold substrate to such a thiol in solution or in the gas phase, a bond between gold and sulfur ($\sim$44 kcal/mol [108]) forms rapidly, typically within seconds to minutes. Following over the next few hours, contributing a significant amount of order to the assembly, is the close-packing of the hydrocarbon tails into a primarily all-*trans* configuration. The adsorption of the molecules extends laterally to accessible substrate, if the exposed thiol is in high enough concentration (with the occupation of $\sim$10^{15} molecules/cm^2). However, the film is restricted from growth normal to the surface because of the molecule's unreactive, methyl-terminated tail, resulting in a chemically passivating film of monomolecular thickness. At low surface coverage, the alkanethiolate molecules lie flat with their hydrocarbon backbones parallel to the gold surface; at higher surface coverages, the molecules begin to stand up, with the hydrocarbon tails tilting approximately 30° from the surface normal and nominally in the all-*trans* configuration so as to maximize van der Waals interactions [109]. In ambient conditions, *n*-alkanethiolate SAMs with $n \geqslant 6$ methylene groups will order; studies in ultra-high vacuum (UHV) have shown that *n*-alkanethiols as short as ethanethiol ($n = 2$) will produce oriented SAMs [110]. SAMs of *n*-alkanethiolates on silver surfaces, for example, are more tightly packed and have less of a tilt angle than those on gold [111]; this is of importance in terms of how the density of the packed SAM can affect the overall utility of the assembly. This tilt angle is determined by the packing density of the headgroups and the optimizing of van der Waals interactions between chains. Exchange of adsorbates within the solution phase will occur in order to form a locally energetically favorable, though kinetically trapped, surface structure. It is possible to move these structures towards equilibrium by exchanging weakly bound molecules and annealing film defects (i.e., increasing domain coherence length) by inserting additional adsorbates from the vapor phase at slightly elevated temperatures [112].

The physical structures and chemical properties of *n*-alkanethiolate SAMs adsorbed onto gold surfaces have been studied by many ensemble averaging techniques to determine the macroscopic characteristics of the monolayer; complementary local probe techniques yield a comprehensive picture of the SAM. Such experimental methods to determine SAM properties include ellipsometry to measure film thickness [22,108,111]; Fourier transform infrared spectroscopy (FT-IR) to examine tilt, order, and gauche defects [22,108,111]; contact angle goniometry to measure the film's hydrophobic character [17]; electrochemistry to probe electron transport through the SAM and to examine structural defects such as pinholes [22,113]; quartz crystal microgravimetry (QCM) to determine the kinetics of monolayer assembly [114–116]; X-ray photoelectron spectroscopy (XPS) to evaluate the composition of the bound species [108]; diffraction (electron/He/X-ray) to investigate the physical structures of assemblies [117]; and temperature programmed desorption (TPD) to

probe the thermodynamic aspects of adsorption and desorption and to determine bond strengths within the assembly [4]. From the early 1990s, scanning tunneling microscope (STM) studies of *n*-alkanethiolate SAMs on gold have shown their organization on the nanometer scale [109,118–121]. Other scanning probes including the atomic force microscope (AFM [122–124]) and the lateral force microscope (LFM) are continuing these studies as well as demonstrating the manipulation of assembled films to make patterned surface structures.

SAMs formed at room temperature are governed by a complex mixture of thermodynamics and kinetics. As mentioned previously, SAMs are typically kinetically trapped at local thermodynamic minima. When imaged with local probes such as the STM (*vide infra*), a variety of local defects are observed. Such defects include substrate vacancies, where ''holes'' that are one atomic layer deep of gold have been formed during the adsorption process. Possible mechanisms for the formation of these are from the ejection of individual gold atoms from the surface layer and subsequent rearrangement of the remaining gold adatoms, an adsorbate-mediated corrosion whereby S–Au bond formations weaken the surrounding Au–Au bonds [125], and from the reconstruction of the gold surface (compressed from extra surface atoms) upon adsorbate binding, where ~2 Au atoms per unit cell are released upon lifting the surface reconstruction and the vacancies coalesce into islands [126,127]. Monatomic step edges, where one atomic layer of gold separates the gold terraces from each other with a height difference of ~2.35 Å, are also present. Defects of the molecular lattice include domain boundaries of the SAM (mismatches in the tilts of the individual *n*-alkanethiolate adsorbates), vacancies within the crystalline lattice of the molecules, and larger grain boundaries.

Several structural features typical of chemisorption of *n*-alkanethiolates on Au{1 1 1} can be seen using the STM as a local probe [121], Fig. 3. Domain
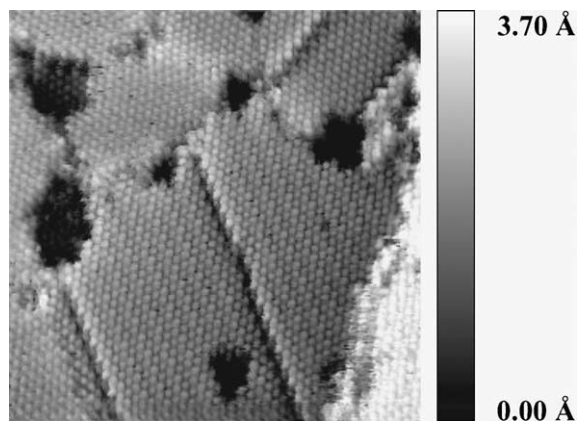
Fig. 3. STM image of a 250 Å × 250 Å area of an *n*-decanethiolate SAM. The molecular lattice is resolved, and the hexagonal close packing of the adsorbates is readily visible. A step edge along with several film defects can be seen, including domain boundaries (protruding and depressed ridged lines) and substrate vacancy islands (dark, circular depressions). Tunneling conditions: $V_{sample} = -1$ V, $i_t = 10$ pA.

boundaries, regions where the alkyl tails may possess either opposite tilt vectors and/ or rotations with those of neighboring adsorbates, stacking faults, or differing sulfur headgroup-lattice registry, can be found. The hexagonal packing of the alkanethio-lates in the $(\sqrt{3} \times \sqrt{3})R30°$ overlayer structure is also visible. The molecules are separated by 4.99 Å, the distance in between the sulfur headgroups bound to the gold substrate. Superlattice structures are also formed [126,128]. Additional defects of the self-assembled film include vacancies in the molecular lattice itself. The structural features and defects shown by scanning probe microscopes such as the STM have shed light on the ability to pattern SAMs in specific locations. While alkanethiolate SAMs are stable surface structures, the adsorption process is highly dynamic and molecules can continue to exchange with other thiol species in solution or in the vapor phase, with many exchange events occurring at structural defect sites. The Au–S bond is strong enough to weaken proximal Au–Au bonds in the lattice beneath the assembly [129], and gold has been found dissolved in solution after desorption [125]. In SAM formation, equilibrium processes that are highly kinetically limited exist between species bound to the surface and free adsorbates (when in the solution phase, these free adsorbates are solvated, and additional energetic factors such as the enthalpy and entropy of solvation play critical roles in the dynamics of adsorption). Substrate vacancy islands, adsorbate vacancies in the molecular lattice, and domain boundaries are critical sites in the monolayer that will enhance and differentiate the effects of post-adsorption processing of the film [130].

The degree of disorder at these sites is increased relative to the rest of the close-packed monolayer, and thus molecules adsorbed at these defect sites are postulated to be less constrained than the surrounding matrix and may have greater conformational mobility. It is highly likely that the solution has increased access to these defect sites, and the presence of solvent may promote the exchange of adsorbed molecules for new species of interest [130]. Step edges are also likely accessible to the solvent and present substrate atoms with low coordination number; thus, these are sites of high probability for adsorption, and molecules that adsorb here may be comparatively more accessible by solvent than their neighbors in the close-packed film. These defect sites within the "host" SAM are postulated to be the most susceptible to exchange to new "guest" adsorbates exposed to the films (*vide infra*).

Alkanethiolate SAMs have been studied in extensive detail by a variety of methods, and with this knowledge we are able to control the types, densities, and distributions of defects of the final monolayer product. The overall quality of the film allows the possibility for further patterning, manipulation and post-adsorption processing, including thermal annealing and backfilling of defects with new adsorbates, which will allow for the characterization (and manipulation) of single molecules with the STM. Exchange of *n*-alkanethiolate molecules for guest adsorbates will occur at defect sites within the SAM, with both host and guest molecules participating in individual and collective exchange events. Infrared spectroscopy studies have shown that multiple exchange events occur, with first a rapid exchange occurring at defect sites such as at grain boundaries, domain boundaries, or at the peripheries of substrate vacancy islands and then with a second, slow exchange, presumably occurring within the domains themselves [110]. We have demonstrated

that molecules can be selectively inserted into SAMs at defect sites, domain boundaries, and step edges, and we use this molecular positioning ability to advantage [62,63,112,130,131]. By capitalizing on the dynamic exchange processes with thiol species in solution, we have begun to characterize isolated molecules that are candidates for nanoelectronic interconnects and functional components with the STM through the positional assembly of these molecules into a surrounding, preformed alkanethiolate matrix [62,63]. Molecules can be brought into the well-defined and understood matrix in extremely low concentrations, and we can elucidate perturbative effects that such molecules introduce when they are studied individually and systematically.

The mobility of adsorbates at surface defect sites is increased as the molecules may not be strongly bound (i.e., sitting on a bridge or on-top site of the Au lattice rather than a three-fold hollow site), they may be located at the edges of large adsorbate domains and thus have a lower interaction energy than their fully-surrounded counterparts, or the molecules may be disordered such that they are susceptible to more interactions with solvent, and thus more prone to exchange or desorption. The ability to reduce the mobility of molecules once they are placed on a surface allows these assemblies to be useful nanoscale structures.

3.2. Organosilane SAMs on SiO₂

Although the majority of this review focuses on the utility and development of the *n*-alkanethiolate SAM, it would be remiss not to mention the role that SAMs of organosilane molecules assembled on silicon dioxide substrates have played in the creation of patterned nanostructures [11]. Organosilanes generally consist of a silicon atom tetrahedrally bound to three similar functional groups (typically short chain alkoxy groups or chlorines), and then to a functional group of interest, which can possess most any functional group listed in Table 1. While the S–Au bond is mostly charge transfer in nature, the "headgroup–substrate" interaction of the silane and SiO_2 surface is quite different; here, the silane molecules condense with native hydroxyl groups adorning the SiO_2 surface, forming a thin layer of covalently linked polysiloxane at the interface, Fig. 4. This small polymer interface is much more thermally stable than its RS–Au counterpart, thus affording greater stability and an extremely robust system. Organosilane SAMs on SiO_2 have been of great utility in the photoresist industry, in which their patterning by energetic beams affords structures that can direct the substrates' topographical etching.

3.3. Alkanethiolates on noble metal surfaces

The structure as well as the placement of alkanethiolate films on surfaces other than gold has been studied and reported. Systems with the same physical and chemical properties of that of the alkanethiolate–gold assembly are desired, as the function of metals more friendly to microfabrication processes would be increased, including platinum [82,132], palladium [105,133], silver [111,134], and copper [111,135]. This area has not yet been explored extensively, but will no doubt turn out
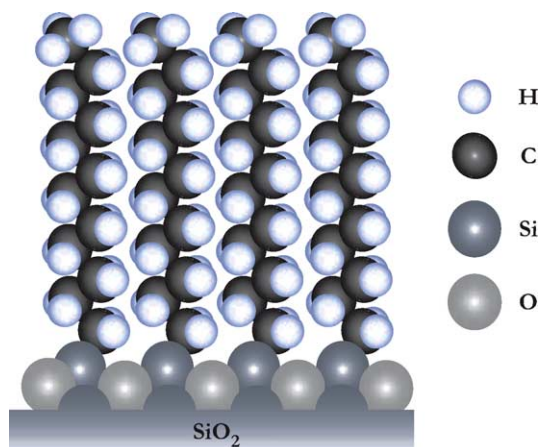
Fig. 4. Schematic of an organosilane self-assembled on a SiO_2 substrate. In order to form a complete monolayer, the silane groups condense with surface hydroxyl groups to form a thin layer of polysiloxane.

to be extremely useful in balancing order and placement of molecules with an ability to create stable and functional nanostructures.

4. Methods of SAM characterization: ensemble and local measurements

A variety of experimental methods have been used to probe the quality and chemical nature of SAMs, from techniques that are macroscopic and average the signal across the entire film, to local probes such as the STM or the AFM, which can examine the structure of the SAM down to atomic resolution and better. Several techniques that have been typically used to characterize SAMs on the macroscopic level, ensemble averaging measurements, are described below. Although local probes provide the most detailed information regarding the structure and order of self-assembled films, by nature they cannot analyze more than hundreds to thousands of square nanometers at a time. It is many different measurements used in concert that present a comprehensive analysis of the film properties. Listed here are the characterization methods that are most pertinent to patterned SAMs, including techniques measuring the macroscopic order of the film as well as local probes that examine the local composition and structure. This section will provide an introduction to how the techniques that can pattern films operate and/or how the patterned films themselves or the substrates underneath them are then characterized.

4.1. Contact angle goniometry

Contact angle goniometry (CAG) has been often used to examine the general hydrophilicity or hydrophobicity of a surface [136], and it has been applied to the surfaces of SAMs as well [17]. The concept of CAG is to place a drop of water (or

other liquid) into contact with the surface, and the angle between the film and liquid droplet is measured. The measured angle reflects the degree of surface order, and can indicate the incorporation of functional groups, for the contact angle changes with varying film composition. For example, CAG can indicate the relative order in an *n*-alkanethiolate SAM as the contact angle will be slightly different from a water droplet resting upon a close-packed, methyl-terminated surface versus a droplet resting upon the disordered and thus exposed methylene tails and interior of the film. For more hydrophilic surfaces (i.e., –OH, –COOH, or –CO$_2$CH$_3$-terminated surfaces), the water droplet will make a smaller contact angle as the water will more effectively wet the hydrophilic surface. Conversely, a drop of a neat liquid such as hexadecane against the surface of an *n*-alkanethiolate SAM will have a very low contact angle, as the hydrocarbon liquid will spread across the surface of the film. While CAG cannot determine the exact molecular composition of a self-assembled monolayer, it can provide a rough estimate of both film quality and overall hydrophilic character. Many groups have used CAG to analyze and to estimate the relative mole fractions of the adsorbates composing mixed SAMs, as the contact angle will change with varying film composition. The "resolution" of the technique is in the many tens of microns range, so that submicron patterns are not readily observed.

4.2. X-ray photoelectron spectroscopy

X-ray photoelectron spectroscopy (XPS) has been used to probe the chemical nature of the SAM; initial studies of SAMs using XPS showed that a covalent bond exists between the sulfur headgroup and the gold substrate, defined the chemical species and oxidation states of constituent atoms in the SAM, and demonstrated that the film is of single monolayer thickness [17,41,108,111,137,138]. Briefly, incident X-rays bombard the sample, and electrons are ejected from the core shells of the atoms within the SAM. Those electrons are collected and dispersed in an analyzer; by measuring the kinetic energies of the electrons entering the analyzer, the binding energies are calculated. These are specific to each element and give indications of the oxidation states of the elements as well. Through angular dependent sputtering experiments, in which the X-rays are focused to destroy through the SAM down to the substrate beneath, the thickness of the SAM can be calculated based on ratios of the substrate signal before and after the presence of the SAM [18]. As it is capable of identifying the elements present and their oxidation states within the SAM, it has been utilized as a powerful diagnostic tool to analyze SAMs once they have been chemically modified.

4.3. Fourier transfer infrared spectroscopy (external reflective)

Fourier-transform infrared spectroscopy (FT-IR) has long been used to measure the vibrational frequencies of bonds within molecules. The vibrational modes of molecules attached to surfaces can also be probed; however, specific surface selection rules exist, and can be used to advantage. Only molecules whose vibrations are

perpendicular to the surface will be detected, as the oscillations running parallel to the surface are effectively cancelled out by the dipole symmetry between the molecules in the film and the metallic substrate. FT-IR has been used to characterize the vibrational modes of SAMs (for both SAMs of *n*-alkanethiols on gold substrates as well as for SAMs of *n*-alkanoic acids on alumina supports); it is most recognized for characterizing the general order within the alkyl matrix of the molecular backbone [22,139]. The alkyl tails vibrate at characteristic frequencies (in the region of $\sim$2800–3000 cm^{-1} [22]); both the breadth of these peaks as well as the frequencies of the vibrations themselves yield a picture of the relative order and fraction of chain defects within the SAM. Should the chains be disordered, the vibrational spectra will show a breadth of the peaks (as the lack of a constraining environment imposed by neighboring alkyl chains will allow a distribution of vibrational frequencies), as well as a slight redshift in vibrational frequency. FT-IR can also identify the presence of particular functional groups by identifying their characteristic vibrational frequencies (i.e., carboxylates, amides, hydroxyls, etc.). Thus, the progress of reactions at SAM surfaces can be followed using FT-IR. Raman spectroscopy has also been used to study SAMs [140,141]; it provides important information about adsorbate orientation through measured vibrations in the v(C–S), v(C–C), v(C–H), and v(S–H) regions, which are often too weak to be detected in IR spectra.

4.4. Electrochemistry

The combination of SAMs and electrochemistry provides for many sophisticated analyses of the film, as well as for controlling the reactivity of the SAM interface by modifying the molecules at the surface. As mentioned above, SAMs have the ability to modify a gold surface; in terms of electrochemistry, the gold substrate is one large electrode. In fact, the presence of an *n*-alkanethiolate film of thickness sufficient to allow for close packing of the chains will provide up to a 99% electrochemical blocking effect (EBE), allowing only 1% of the current that could occur before SAM adsorption [22,142]. "Pinhole" defects that occur during SAM formation allow access to the underlying Au substrate, and because they are of such low density (with their fractional surface coverage $\leqslant 0.01$), can serve as an array of ultra-microelectrodes [143,144].

Generally, the SAM-modified gold electrode is placed into an electrochemical cell with counter- and reference electrodes. To measure the EBE of the SAM, a freely diffusing species capable of forming a reduction–oxidation pair with the gold surface is placed in the electrochemical cell along with an electrolyte; common choices include $Fe(CN)_6^{+3/+2}$ and $Ru(NH_3)_6^{+3/+2}$. The metal ions can only be reduced or oxidized at the gold surface through pinholes and other defects in the monolayer film, where the species can penetrate through the SAM and access the electrode underneath [143]; such pinholes have been shown to be permanently passivated by the electrochemical polymerization of phenol [145]. Other electrochemical measurements that have been performed on SAMs include the measurement of changes in the electrode's capacitance (which decreases as a function of the thickness of the organic

layer adsorbed atop the gold surface), as well as measurements of the rates of electron transfer through SAMs of varying atomic constituents.

For electron transfer studies through the film, the redox couple is often covalently linked to the monolayer itself. For example, probes such as ferrocene (Fc) and pentaaminepyridine ruthenium are synthesized so as to be at the termini of the adsorbates, thus presenting themselves at the external SAM interface. An alkyl matrix lies underneath the Fc probes in order to form a close-packed SAM that spatially separates them from the surface (this alkyl matrix has been manipulated to contain other functional groups in order to probe the individual contributions of the methylene matrix or other groups to the electron transfer through the film). For example, electrons can be drawn from an immobilized Fc down to the gold electrode with positively applied potentials [113]. The rate at which these electrons travel can be measured, and the rates at which the electrons move through the film are material-dependent. For example, by controlling the spatial distribution of electroactive adsorbates (i.e., alkanethiolates terminated with Fc) diluted within methyl-terminated alkanethiolates, highly sensitive ultra-microelectrode arrays can be incorporated into a SAM. The presence of conjugated groups in the interior of the film (such as phenylene–vinylene, phenylene–ethynylene, alkene, or alkyne moieties) can greatly accelerate the electron transfer through the film, as electrons can move through delocalized pathways as opposed to σ pathways in alkyl networks [25,49]. As electrons can be moved controllably through a SAM, electrochemistry can also be used to reduce or to oxidize pendant groups at the solution–film interface that may be poised for further reaction [65,146,147], as well as to reduce or to oxidize the headgroup so as to desorb the molecule in order to perform post-adsorption processing on the SAM [148–150].

4.5. Scanning probe microscopes

Fundamental studies of the stability of SAM structures are critical, as they will lend insight into the integrity of the final patterned structures. Factors including mobility of the *n*-alkanethiolates once adsorbed to the surface, their thermal stability, and their resistance to a variety of solvent and other environmental conditions will ultimately determine the fate of the applications of these SAMs. For example, should two or more adsorbates be patterned on a surface, perfect edge resolution in their phase boundaries will cease to be important if the adsorbates are mobile and interdiffuse once on the surface. Scanning probe microscopes have greatly assisted in the patterning of SAMs by analyzing the spatial distribution of adsorbates across a surface. For comprehensive reviews of the mathematical and physical treatments of the STM, related scanning probe microscopes and their capabilities, the reader is referred to several outstanding texts [151,152].

4.5.1. Scanning tunneling microscopy

Since the early 1990s, the STM has been used to image SAMs of *n*-alkanethiolates adsorbed on gold surfaces. The STM has been able to provide insight into the mechanism of SAM formation as well as to elucidate important structural features

that lend SAMs their integrity as surface-stable entities. Invented in the early 1980s, the STM was designed to probe the local electronic and physical structures of surfaces [153]; to date, the STM has imaged a variety of materials including metals, semiconductors, insulators, organic molecules, and biomolecules.

Rastering the tip across the sample surface generates an image of electronic features, and the resulting image is a convolution of both the topographic and electronic features of tip and sample, Fig. 5 [154]. The tunneling current drops exponentially upon moving the probe tip away from the surface, typically with a decay constant of 1–2 Å^{-1}, which describes how the wavefunction of the electron falls off as a function of distance. Thus, the STM possesses high lateral resolution of features as the majority of tunneling occurs from the endmost atom of the tip, and proximal atoms or other tip features capable of tunneling contribute much less to the total tunneling current due to their increased distance from the surface. Depending upon the geometry of the probe tip, it is not uncommon for jagged metal features (microtips) to be present that participate in the tunneling current as well and serve to convolute artifactual features with the electronic and topographic information that constitute a STM image.

When an electron tunnels from a metal tip, through an alkanethiolate SAM, and to the metal substrate underneath, it is traveling through two different regions; it tunnels through the gap from the end of the tip to the film interface (whether air or vacuum), and then through the film to the gold, Fig. 6. Each region has its own thickness (labeled as d_{gap} or d_{SAM}), and its own transimpedance, G_{gap} with decay constant α and exponential prefactor A, and G_{SAM} with decay constant β and exponential prefactor B. Depending upon the chemical nature of the SAM itself, the decay constant β changes, leading to different tunneling characteristics (and thus electronic contrast) between two types of materials present on a surface [21]. It is expected that the transmission characteristics of the gap are constant, and thus any
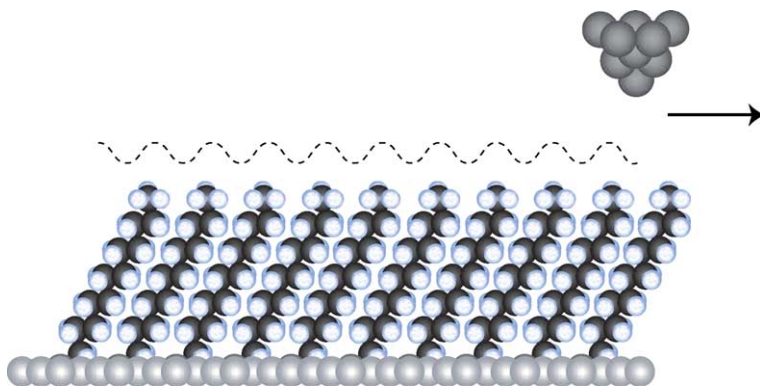

Fig. 5. Schematic of a scanning tunneling microscope tip rastering across the surface of an *n*-alkanethiolate SAM. Operating in the constant-current feedback mode, the metal STM tip extends and retracts in order to maintain a constant amount of tunneling current between tip and sample.
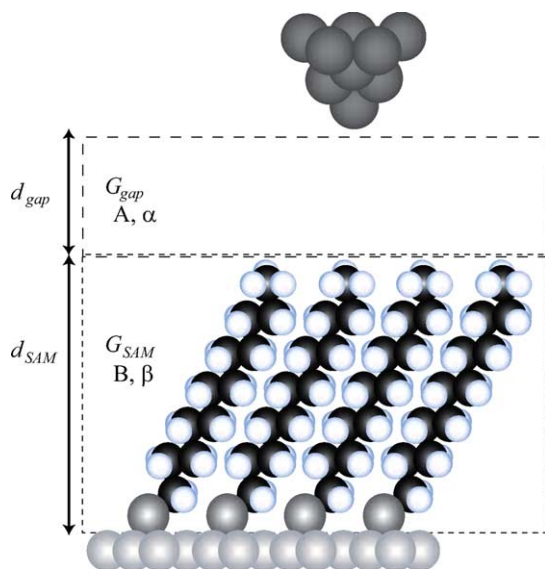
Fig. 6. An electron tunneling through a SAM can be described by a two-layer tunneling junction model, in which the electron moves through two regions, each with its own gap impedance that is a function of the material present. Adapted from Ref. [21], and reproduced with permission of the American Chemical Society.

changes in the electronic image and information of the SAM (for like functional groups, identically presented) are material-dependent.

When operating at low tunneling currents, an STM can resolve the molecular lattice of an *n*-alkanethiolate SAM, imaging the terminal methyl groups and showing their hexagonal close packing. A typical image of an *n*-decanethiolate SAM on Au{1 1 1} shows the individual molecules resolved in their superlattice configuration, as well as several film and substrate defects, Fig. 3. The particular spatial distribution of molecules on a surface can be imaged with STM.

4.5.2. Atomic force microscopy

While the STM is an incredibly powerful tool that examines the electronic and physical behaviors of molecules and their assemblies on the nanometer scale, it is only one of many scanning probe techniques that are rapidly changing our understanding of molecular-scale behavior and that will ultimately design and shape the research and structures in fields including biomolecule-based assembly and molecular nanoscience. The atomic force microscope (AFM) has greatly enriched the analysis of surfaces and surface-bound assemblies [155–157]. Whereas the STM requires that a sample be conducting, semiconducting, or at least conducting enough to dissipate charge quickly and avoid changing the potential difference between tip and substrate, the AFM has no such requirement. The principles of the AFM's operation have led to the instrument's many permutations to obtain much more than
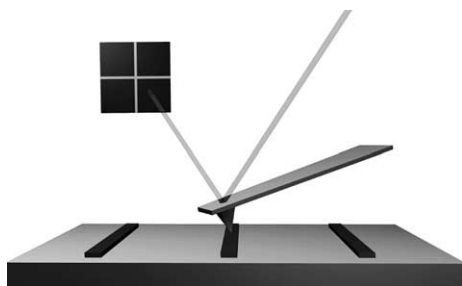
Fig. 7. Schematic of an AFM's operation. A sharp tip resides at the end of a cantilever, rastering along a surface, detecting differences in features (illustrated here as dark stripes). The deflection of the AFM tip as a function of surface properties is recorded by shining a laser beam upon the cantilever's back, which is then sent to a position-sensitive photodiode.

merely topographic information. Briefly, the AFM typically operates by rastering a sample against a sharp tip that is connected to the end of an oscillating cantilever. Attractive and repulsive forces between the tip and the chemical environment of the sample will cause the cantilever to deflect to a certain degree, as will variations in pure topography, Fig. 7.

Feedback mechanisms and thus measurement sensitivity for the AFM include forces due to magnetism, friction, surface charge or potential, or capacitance. This enables the development of scanning probes that are specific to molecular-scale properties; there are several modes of AFM operation that have been chosen to create and to characterize patterned SAMs at the nanoscale, including lateral force microscopy, which can distinguish between different chemical functionalities on a patterned surface due to tribological differences [158,159]; conducting probe AFM, where the tip has been coated with a metal that can send current through a SAM to measure either its conductance or to desorb adsorbates reductively in particular patterns, magnetic force microscope, which has probed the magnetic properties of atomic-scale structures and ultra-thin films [160,161]; the electrostatic force microscope, which has been used to probe the local domain structure of ferroelectric crystals as well as study the structures and charges of semiconductor surfaces [162–165]; the scanning capacitance microscope, which has been used to examine two-dimensional dopant profiling in semiconductors for integrated circuits [166,167]; and the chemical force microscope to examine the adhesive and frictional forces of surfaces [168,169].

4.5.3. Lateral force microscopy

The lateral force microscope (LFM) is a variant of the AFM tuned to respond to tribological differences of the surface. This has been useful for determining the spatial distribution of multiple adsorbates on a surface that differ in terminal groups in order to predispose a portion of the surface to a particular reactivity. In addition to topographic features that change the position of the cantilever, the cantilever can also experience twist (torsion) from changes in the tip-sample interaction. This
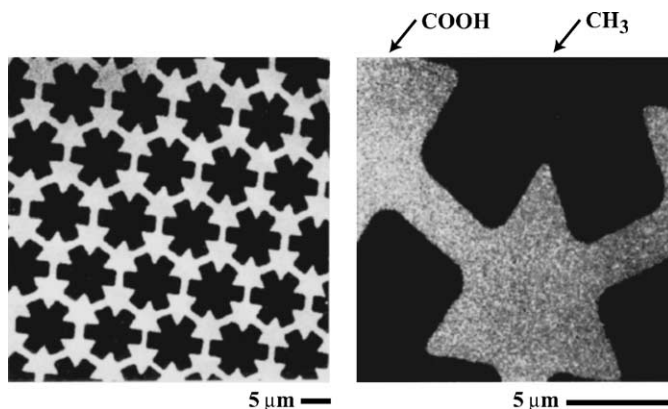
Fig. 8. A lateral force microscope image contrasting the individual domains of carboxylic acid-terminated and methyl-terminated alkanethiol adsorbates patterned on a gold surface; the areas of acid termini and methyl termini are labeled. The acid-terminated regions are shown as brighter due to stronger tip-sample interactions, as a greater voltage is being required to balance the lateral force of the cantilever. Adapted from Ref. [158], and reproduced with permission of the American Chemical Society.

torsion also affects the position of the cantilever, and thus the signal of the laser on the photodiode. For LFM operation, the difference between the signals from the left and right sides of the photodetector is registered as a lateral force, and a relatively larger positive difference between the left and right sides of the photodetector corresponds to greater lateral force [158]. For example, within an n-alkanethiolate SAM, the LFM can easily distinguish between adsorbates terminated with carboxylic acid groups that have been patterned amongst methyl-terminated alkanethiolates, Fig. 8 [123,158]. The friction between the tip and sample will be higher in the acid-terminated regions, and the tip will glide easily in the relatively low friction methyl-terminated regions; the differences in lateral forces exerted on the probe tip in these regions are recorded. The LFM can provide excellent chemical contrast between such differing molecules, and can show with nanometer-scale precision the placement of different molecules on a surface.

5. Formation of multicomponent self-assembled monolayers

The patterning of SAMs involves deliberately placing molecules into specific spatial arrangements or distributions on a surface. Differing self-assembling components are often separated into domains once organized, either by spontaneous assembly governed by thermodynamics and kinetics at the local scale, by their direct placement in a stepwise fashion, or by post-adsorption processing of the individual components. Changing the relative mole fractions of adsorbates on the surface may necessitate changing patterning schemes in order to effect the desired structure. The following sections discuss efforts to pattern molecules on a surface, including solution-phase coadsorption, from which it can be determined how molecules interact

with both similar and dissimilar adsorbates on the surface at the local level, placement of molecules into pre-existing SAMs through defect-mediated exchange as well as their positive placement on the surface, where the level of control is inherently higher but often with sacrificed resolution of feature boundaries. As these kinetically trapped systems are not at equilibrium, they are susceptible to further manipulation by a variety of methods.

5.1. Spontaneous phase separation

When two differing adsorbates are mixed in solution and then exposed to a substrate, both species will adsorb on the surface. If the species differ enough in molecular composition, they will aggregate into homogeneous domains so as to maximize self–self interactions through van der Waals, hydrogen bonding, or other interactions. However, many complex factors arise when attempting to pattern molecules on a surface by simple solution-phase coadsorption. It is important to note that the relative fractional surface coverages of the molecules will not necessarily be that of the coadsorption solution; for example, a 1:1 mole ratio of adsorbates A and B will not necessarily yield a surface composition of 1:1 A:B, an observation supported by contact angle, scanning probe microscopy and electrochemical studies [40,51,170–173]. Factors that affect the competition for the surface include the relative solvation of the adsorbates by the solution, the sticking probability of each molecule, and the degree of interaction between the molecules once they are adsorbed. Molecules that may be better solvated may not adsorb as quickly to the surface, while the comparatively less soluble molecules may either aggregate in solution or aggregate together on the surface, both situations where the molecules' self-interactions are maximal. The enthalpies of these intermolecular interactions as well as the minimization of poor cross-interactions provide strong driving forces for the separation of multiple adsorbates into their homogeneous domains.

STM has greatly assisted in understanding the placement of molecules coadsorbed on surfaces, and thus how surfaces can be manipulated once the adsorbates are placed on the surface. From STM information at the nanometer scale, more complicated nanostructures have been created. Numerous spontaneously component-separating SAM systems have been studied, using both local probes as well as ensemble-averaging measurements. Such systems include the coadsorption of short- and long-chain alkanethiols [170,174,175], molecules that differ both in chain length and functional groups (i.e., 3-mercaptopropanol and *n*-tetradecanethiol [176]), molecules of similar length but with differing terminal groups (i.e., *n*-hexadecanethiol and its methyl ester analog [120], *n*-undecanethiol and 11-mercaptoundecanoic acid [50]) and molecules of similar length but with differing, buried functional groups (i.e., 3-mercapto-*N*-nonylpropionamide and *n*-decanethiol [172,173]). However, molecules of similar enough composition will not phase separate if formed at room temperature from the same solution (*n*-decanethiol and *n*-dodecanethiol [130]). The likelihood of preferential exchange is decreased, as the energies of solvation and exchange will be similar between the two adsorbates. Their limited mobility from energetically similar van der Waals interactions prevents them from moving great distances,

though if the substrate is still immersed in solution, they are free to exchange off of the surface and then back on again.

5.1.1. Variation of the alkyl chain

Some of the first phase-separated SAMs reported were formed from the coadsorption of *n*-alkanethiols that differed only in the lengths of their alkyl chains [18,138,174]. Whitesides and coworkers reported contact angle measurements, ellipsometry, and XPS data of SAMs formed from differing ratios of adsorbates; they showed that SAMs of known adsorbate concentrations could be reproducibly formed. Using their ensemble measurements and modeling the adsorption events and intermolecular interactions, they inferred that single-component SAMs were the lowest energy structure of a SAM exposed to a solution of two adsorbates. Scanning probe microscopy data, however, has shown the presence of nanoscale domains of adsorbates separated into two components [120]. Both local probe and ensemble-averaging measurements agree, however, that the adsorbate domains that exist on the surface tend towards homogeneity. These experiments of Whitesides and coworkers provided evidence for the fact that the ratio of adsorbates in solution does not mirror that of the surface-bound adsorbate composition. The scanning probe measurements indicated that these multicomponent films do not typically reach equilibrium [120].

5.1.2. Variation of the terminal functional group

Separation of two adsorbates into their homogeneous domains on a surface has been observed when the components' tail groups are vastly different in polarity. Methyl-terminated alkanethiolates have been shown to be essentially miscible with –OH-terminated alkanethiolates when the chain lengths are similar [18]. In fact, many of the early phase separation studies by Whitesides and coworkers were performed using –OH-terminated and –CH$_3$-terminated adsorbates in order to probe molecular cross-interactions as well as to analyze how each adsorbate responded to hydrophilic and hydrophobic contact angle measurements (the terminal groups extending into or retracting from the probing solution). In fact, even SAMs composed of –CH$_3$- and –COOH-terminated alkanethiolates have been shown to be slightly miscible (undecanethiolate and 11-mercaptoundecanoic acid), although domains of each molecule are readily observed [177].

STM studies have shown that coadsorbed SAMs of *n*-hexadecanethiol and the corresponding methyl ester will phase separate into homogeneous, nanoscale domains, Fig. 9 [120]. STM has also shown that molecules with vastly differing functionality (i.e., both terminal group as well as chain length) will separate into their homogeneous domains on the surface; Fig. 10 shows the phase separation of short-chain, carboxylic acid-terminated and long-chain, hydrophobic alkanethiolates.

5.1.3. Variation of the buried functional group

There are many instances in which phase separation can be driven in binary-component SAMs by changing the terminal functional group between the two adsorbates. However, phase separation can also occur if the molecules possess differing
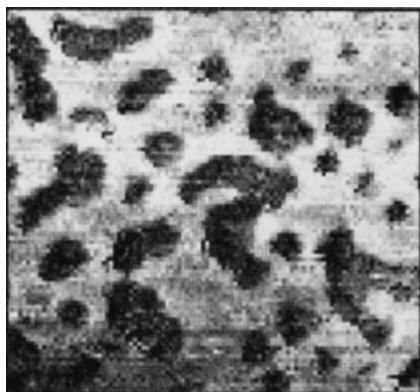
Fig. 9. STM image of a 440 Å×410 Å area of a phase separated SAM of *n*-hexadecanethiol (HS(CH$_2$)$_{15}$CH$_3$) and its methyl ester derivative (HS(CH$_2$)$_{15}$CO$_2$CH$_3$). The relative mole fraction of the adsorption solution was 1:3 thiol:ester. Adapted from Ref. [120], and reproduced with permission of the American Chemical Society.
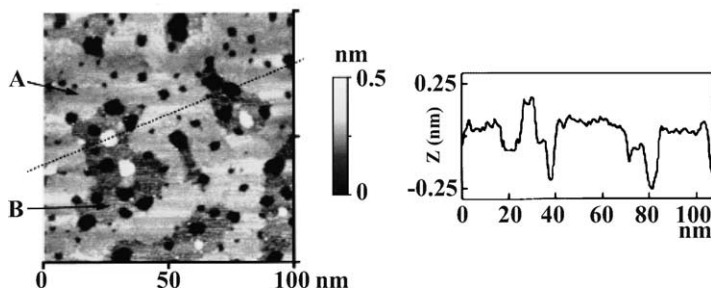

Fig. 10. STM image of a binary SAM composed of *n*-decanethiolate and 3-mercaptopropionic acid; the adsorption solution was composed of 10:90 *n*-decanethiol:acid. Domains labeled as 'A' are of *n*-decanethiol, and domains labeled as 'B' are of the carboxylic acid. A cross-sectional profile across the SAM, showing the relative difference in topography of the two domains, is shown at the right. Tunneling conditions: $V_{sample} = +0.37$ V, $i_t = 1$ nA. Adapted from Ref. [178], and reproduced with permission of Elsevier Science.

functional groups that are buried near the film–metal interface. Phase-separated SAMs have been reported where the adsorbates are a mixture of *n*-alkanethiolate and an adsorbate containing an amide group buried down near the sulfur head-group, Fig. 11 [172,173]. Amide-containing molecules are capable of hydrogen bonding to their nearest neighbors, providing a high enthalpic driving force for phase separation when adsorbed on the surface. The increasing interaction energies with molecules containing multiple amide groups further assists in imparting order (and thermal stability as well) to the assembly, and the directionality of the hydrogen bond can assist in aligning molecules (white arrow in Fig. 11). These hydrogen bonds can assist in forming the sharpest of boundaries between domains, those that are
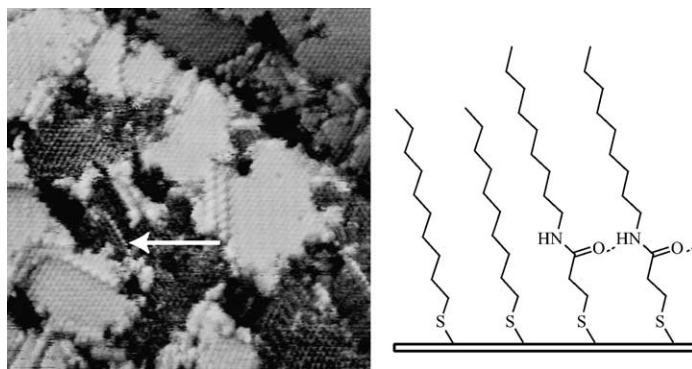
Fig. 11. STM image of a 220 Å × 220 Å area of a binary component SAM formed of equal mole fractions *n*-decanethiol and 3-mercapto-*N*-nonylpropionamide. The adsorbates phase-separate into domains (the amide-containing molecules appear as topographic protrusions). Substrate vacancies and a monatomic step edge (upper right corner) can be seen. The white arrow points to a linear array of amide-containing molecules, consistent with their aligning to optimize intermolecular hydrogen bonding interactions. Tunneling conditions: $V_{sample} = +1$ V, $i_t = 1$ pA. A schematic of the phase-separated domains is shown at the right; guides are shown between the carbonyl oxygens and amide protons to show the directionality of hydrogen bonding across the array. Adapted from Ref. [172], and reproduced with permission of the American Chemical Society.
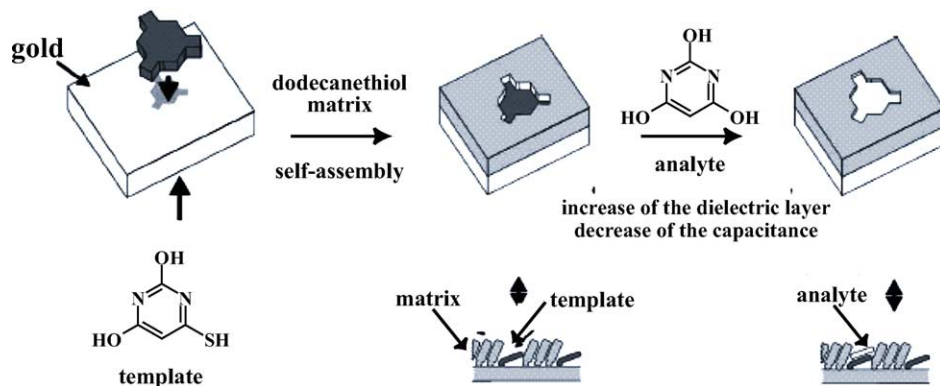
Fig. 12. Schematic of a molecularly imprinted sensor (here, for barbiturate) showing the coadsorption of thiobarbiturate and an *n*-alkanethiol. The thiobarbiturate serves as a template for the barbiturate analyte, and functions as a "spreader-bar" to preserve the templated shape of the analyte by preventing the lateral diffusion on the surface-bound alkanethiolates. Taken from Ref. [150], and reproduced with permission of Wiley–VCH.

only one molecule wide. This propensity may be useful in exploiting intermolecular interactions for the precise placement of molecules in films.

The principles of phase separation, whether by segregation of electroactive molecules serving as ultra-microelectrodes or by the aggregation of molecules imparting a particular physical property to the surface, have been applied to make SAM-based

sensors. Sensors for barbiturate and cholesterol have been created by capitalizing on the phase separation between such analytes and *n*-alkanethiolates. Two-dimensional "molecular imprinting" has been used to create templates for analyte adsorption by coadsorbing an *n*-alkanethiolate with the analyte's thiolated derivative (i.e., thio-barbiturate, thiocholesterol) [179,180]. The thio-analytes orient themselves in the plane of the gold substrate, and the alkanethiolate molecules orient themselves around the template molecules, reinforcing the orientation of the templates on the surface, Fig. 12. The fact that the coadsorbed analyte derivatives have thiol groups prevents them from moving on the surface (serving as a "spreader-bar," preventing the lateral diffusion and coalescence of the alkanethiolates and thus destroying the imprinted shape of the template molecules). The analytes of interest, such as barbiturate or cholesterol, bind atop the template with remarkable chemical specificity, as they are almost identical in shape; the number of binding events is monitored by measuring changes in the overall capacitance of the assemblies (as the capacitance decreases with increasing film thickness [179]).

5.2. Directed assembly leading to component separation

It has been shown that *n*-decanethiol and *n*-dodecanethiol will not phase separate if coadsorbed from solution onto a surface at room temperature, Fig. 13; the two can be separated into their homogeneous domains by post-adsorption techniques such as thermal processing and backfilling (*vide infra*).

5.2.1. Thermal processing of SAMs

Bumm et al. have demonstrated that it is possible to direct the assembly and consequent separation of adsorbates by thermally processing homogeneous, single-component SAMs followed by their exposure to new adsorbates in order to form separated, binary-component SAMs [130]. Domains of adsorbates can coalesce and the number of substrate vacancy islands can be reduced by heating the SAM in hot ethanol; the defect density is even further reduced by heating the SAM in a solution of excess adsorbate, Fig. 14. Fig. 15 shows a binary-component SAM that has been formed by thermally annealing an *n*-decanethiolate SAM in hot ethanol, followed by backfilling it with *n*-dodecanethiolate from solution. The post-adsorption thermal processing of the decanethiolate molecules in neat ethanol gives the assembly thermal energy to draw the adsorbates together, while simultaneously inducing desorption of weakly bound *n*-decanethiolates. Therefore, vacant lattice sites exist for the introduction of new adsorbates, affording a binary, component-separated SAM.

5.3. "Host–guest" self-assembled monolayers

In an effort to understand the intermolecular dynamics of adsorbates on surfaces and to comprehend fully the mechanisms of adsorption and exchange of adsorbates in solution with those on surfaces, molecules can be placed on a surface at low fractional surface coverage within a pre-existing matrix of a SAM that has already
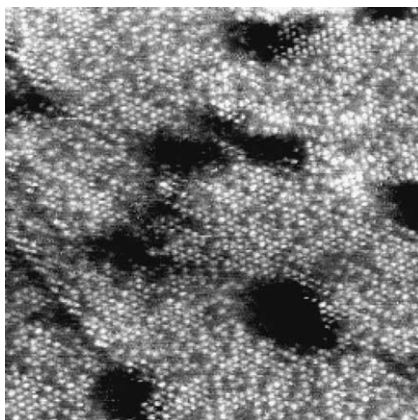
Fig. 13. STM image of a 200 Å×200 Å area of a binary SAM composed of *n*-decanethiolate and *n*-dodecanethiolate. The surface shows a random spatial distribution of molecules on the surface, when they are coadsorbed from solution at room temperature. The *n*-dodecanethiolate molecules appear as the brighter spots due to the topographical difference of two –CH_2– groups, and the *n*-decanethiolates appear as the lower lying gray regions. Each spot corresponds to a terminal –CH_3 group of an individual adsorbate. Tunneling conditions: $V_{sample} = +1$ V, $i_t = 2$ pA. Adapted from Ref. [181], and reproduced with permission of the American Vacuum Society.
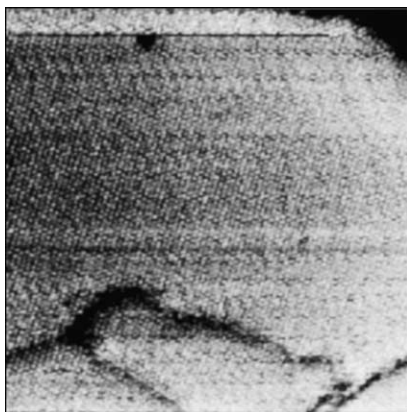
Fig. 14. STM image of a 400 Å×400 Å area of a thermally annealed SAM of *n*-dodecanethiolate. The SAM was formed at room temperature and then was heated in a solution of *n*-dodecanethiol for 1 h at 78 °C; many surface defects such as substrate vacancies were annealed, leaving large domains of adsorbate. Tunneling conditions: $V_{sample} = -1$ V, $i_t = 10$ pA. Taken from Ref. [130], and reproduced with permission of the American Chemical Society.

formed. Through these studies, it has been shown that incoming ("guest") molecules will insert into a ("host") SAM at its local defect sites (discussed in Section 3.1), by exposing the preformed SAM to a solution of guest adsorbate that is of low concentration (typically 0.1–0.5 mM) and for short periods of time (minutes to hours)
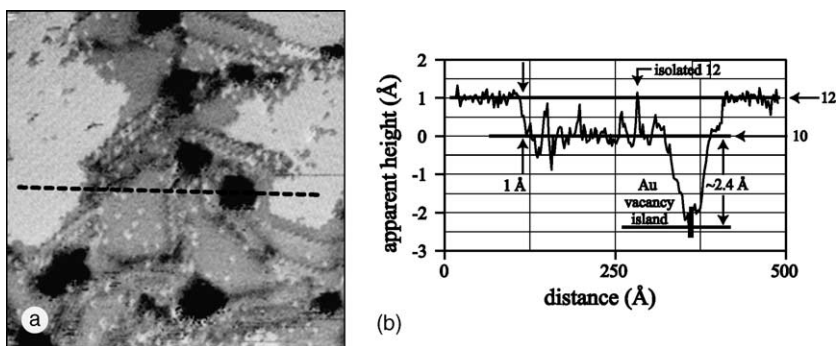
Fig. 15. (A) STM image of a 500 Å×500 Å area of a phase separated SAM composed of n-decanethiolate and n-dodecanethiolate. The two adsorbates are in homogeneous domains; this "mosaic" SAM was formed by creating a SAM of pure n-dodecanethiolate, followed by thermal desorption in neat ethanol, and then re-exposing the substrate to a solution of n-decanethiol. Tunneling conditions: $V_{sample} = -1$ V, $i_t = 10$ pA. (B) A topographical line scan (represented by the dashed line in (A)) showing the relative heights of the adsorbates, as well as showing the depth of the gold substrate vacancies. Adapted from Ref. [21], and reproduced with permission of the American Chemical Society.
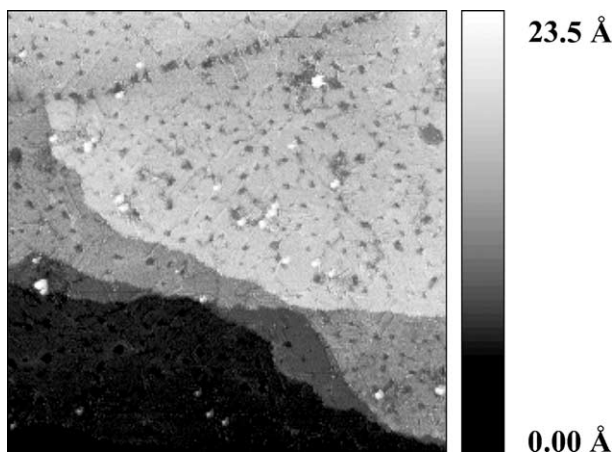
Fig. 16. STM image of a 1500 Å×1500 Å area of an n-dodecanethiolate SAM into which a small mole fraction of an oligo(phenylene–ethynylene)-functionalized (OPE-) thiol has been inserted (appearing as higher topographically due to their higher conductance as compared to the insulating alkyl host matrix). The inserted guest molecules insert into the host SAM at surface defects and features such as step edges, domain boundaries, and substrate vacancy islands. Tunneling conditions: $V_{sample} = -1.4$ V, $i_t = 0.2$ pA. Adapted from Ref. [63], and reproduced with permission of Science.

[62,63,130,131,182]. Fig. 16 shows both single and small groups of conjugated molecules that have inserted into a preformed matrix of n-dodecanethiolate. It is possible to insert pairs of molecules by inserting (symmetric or asymmetric) disulfides into a host matrix.

The fractional surface coverage of molecules inserted into host SAMs is neither only a function of the concentration of guest molecule exposed to the host SAM nor is it simply a function of the time of exposure. The defect density of the host SAM is of significant importance as well, for guest molecules tend to insert into the host SAMs at defect sites. It would then be expected that a greater defect density within the host matrix would lead to increased fractional surface coverage of guest molecules. Several studies have been performed to manipulate a film's defect density, including (a) increasing the defect density by adsorbing the SAM for a short period of time, thus limiting slower ordering processes, (b) decreasing the defect density by backfilling the host matrix with adsorbates from the gas phase [112,182], and (c) warming the substrate to allow step flow motion to annihilate domain boundaries and substrate vacancies. When the defect density of a SAM is high (i.e., SAMs formed by exposure of the gold to *n*-alkanethiolate for 5 min), molecules will insert at higher fractional surface coverage [63,182]. Conversely, if guest adsorbates are inserted into the SAM and then the SAM is backfilled with additional adsorbate from the gas phase, then the fractional surface coverage decreases, Fig. 17. STM images show that the molecules inserted from the gas phase once the host–guest assembly is formed insert in the same locations as the guest molecules (step edges, domain boundaries, etc.), and provide a reinforced network of molecules surrounding the guest [112,182]. The images also show that the molecules inserted from the gas phase remain phase separated from the SAM adsorbates of the host matrix.
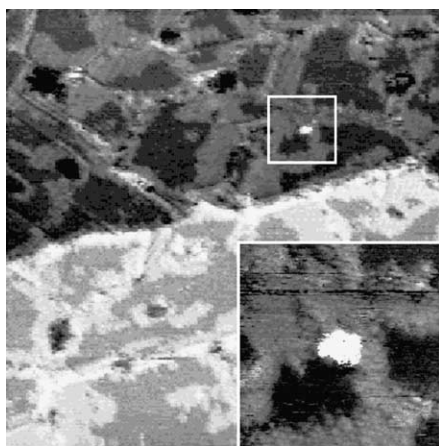
Fig. 17. STM image of a 800 Å×800 Å area of a SAM of an *n*-decanethiolate into which an OPE-functionalized thiol has been inserted. Once the host–guest SAM assembly had formed, the SAM was backfilled with *n*-dodecanethiolate in the vapor phase to fill in all lattice sites and to improve the quality of the host matrix by thermally annealing some film defects. The inset image is 135 Å×135 Å, showing the inserted molecule (brightest) surrounded by a mosaic network of vapor-annealed *n*-dodecanethiolate and the host *n*-decanethiolate. Tunneling conditions: $V_{sample} = +1$ V, $i_t = 10$ pA. Adapted from Ref. [182], and reproduced with permission of the Japan Society of Applied Physics.

5.4. Electrochemical manipulation of adsorbed thiolates

When two or more substantially different adsorbates are mixed in solution and exposed to a substrate to form a SAM under the same conditions, there will typically be phase separation of the components to some extent in order to maximize self-interactions. The degree to which molecules phase separate on a surface can be tuned by their chemical composition and by their relative mole fraction in the adsorption solution. Electrochemistry can be used to manipulate the adsorbates themselves by electrolytically cleaving the Au–SR bond at the interface, resulting in a free thiolate and Au^0; the proposed mechanism is RS–Au + e$^-$ → RS$^-$ + Au [183–185]. Thiols are typically displaced from metal electrodes by applying reductive potentials (equation above), yet it is also possible to strip them from surfaces using oxidative potentials, Fig. 18 [150,183,186,187]. Different thiols have different reductive potentials, varying from −0.75 V (for short mercaptoalkanoic acids) to −1.12 V (for *n*-hexadecanethiol, both peak potentials vs. Ag/AgCl electrodes) [149]. Therefore, it is possible to desorb individual, small groups, or domains of thiols selectively without desorbing others, should two or more thiols be coadsorbed on a gold surface.

Electrochemical manipulation of SAMs can be used to enhance phase separation of binary-component SAMs [188]. For example, two adsorbates whose phase separation might be minimal on the local scale can be separated into compositional domains by starting with a widely phase separating system (*vide supra*, with adsorbates that differ in both terminal functionality as well as their alkyl chain length), desorbing one of the components electrochemically by selecting the appropriate reduction potential, and then backfilling with a new (third) adsorbate of interest. This approach has been demonstrated by Kakiuchi et al. in making phase-separated SAMs of *n*-undecanethiolate (UDT) and *n*-hexadecanethiolate or 11-mercaptoundecanoic acid, starting from binary SAMs composed of UDT and 3-mercaptopropionic acid (3-MPA) [171,189]. They selectively desorbed the 3-MPA as it has a less negative reduction potential than the UDT and then backfilled with either *n*-hexadecanethiol or 11-mercaptoundecanoic acid. Using STM, they observed that
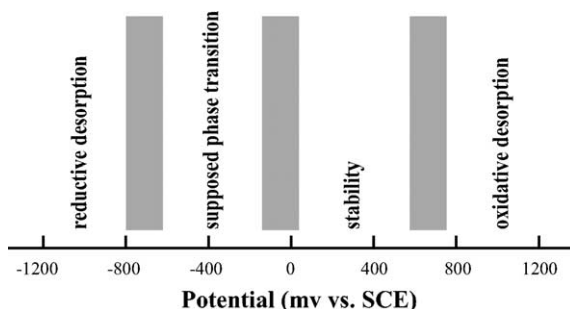

Fig. 18. Various electrochemical potentials for the stability of *n*-alkanethiolates adsorbed on gold electrodes. All potentials shown are reported versus a saturated calomel electrode (SCE). Adapted from Ref. [150], and reproduced with permission of Elsevier Science.
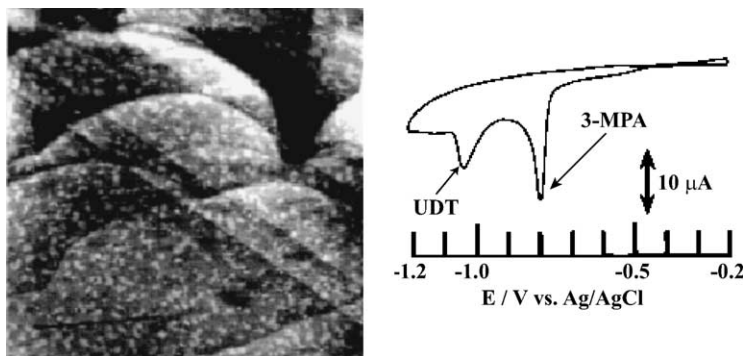
Fig. 19. STM image of a 4000 Å × 4000 Å area of a phase-separated SAM of *n*-undecanethiolate and 3-mercaptopropionic acid (9:91 UDT:3-MPA) adsorbed on a Au{1 1 1} substrate. The undecanethiolate molecules are the protruding islands (average domain size is 10–20 nm). A cyclic voltammogram shows the reductive desorption peaks (and potentials) of the two adsorbates, showing that the 3-MPA molecules will be selectively removed under a slightly less negative applied electrochemical potential. Tunneling conditions: $V_{sample} = +1.5$ V, $i_t = 8$ pA. Adapted from Ref. [171], and reproduced with permission of the American Chemical Society.

the relative sizes of the domains do not change significantly during and after the desorption and backfilling processes, Fig. 19. This is especially important, as adsorbates that would ordinarily be miscible on the surface when coadsorbed from the solution phase can be manipulated to be partitioned into two separate and distinct domains. However, adsorbates on the surface do possess somewhat limited mobility, and the possibility exists that molecules that have been artificially phase separated into differing domains may diffuse slowly at the interphase, blurring feature boundaries [190]. It may be possible to reduce such motion if the adsorbates possess strong intermolecular interactions, such as in the amide-containing molecules; additionally, the tightness of the SAM matrix can assist in preventing molecular diffusion, as diffusion is not observed within domains [130]. Therefore, molecular interdiffusion across the surface could be countered either by the necessity of concerted motion from its surrounding adsorbates or by the energy of the interactions.

Several applications have emerged from the electrochemical manipulation of SAM adsorbates. The reductive desorption of phase-separated alkanethiolates has also been employed in order to backfill with thiolated nucleic acids for the purpose of creating ultra-sensitive, sequence-specific detectors of nucleic acid hybridization [191]. Patterned arrays of enzymes have been fabricated by reductively desorbing particular segments of alkanethiolate SAMs with the scanning electrochemical microscope (SECM) [192]. Reductive desorption in predetermined locations by the SECM tip leaves a bare gold surface; amino-terminated thiol was backfilled in the regions and the substrate was exposed to a solution of horseradish peroxidase which was immobilized selectively in the amino-terminated regions. The enzyme retained its activity, as demonstrated by reducing H_2O_2.

Several methods of controlling the spatial distributions of adsorbates from the solution phase have been discussed; however, it is possible to pattern adsorbates directly on a surface through their direct placement. The following sections discuss various patterning methods through positive placement.

6. Patterning self-assembled monolayers using soft lithography

It has been just a decade since Whitesides and coworkers introduced the field of "soft lithography" [98]. Since that time, there have been numerous studies demonstrating this family of techniques and its versatility in constructing architectures at the nanometer to micrometer scales [193–196]. Soft lithography describes how soft materials such as flexible, elastomeric polymers are used as the primary means of transferring and fabricating features into and onto substrates without the assistance of energetic beams (i.e., photons, ions, electrons). A variety of materials, surfaces, and chemical systems of interest can be used [193]. The chemical systems generated by soft lithography are not damaged by the tools used to create them, and thus can be integrated easily into systems where tools such as energetic beams would be too destructive. In particular, these methods have found considerable usage in patterning SAMs; initially, such SAM patterning served as a means to an end, in which the patterned SAMs served as sacrificial resists to pattern the substrate underneath them selectively. There is a vast body of literature available that describes in detail the various soft lithography techniques, namely microcontact printing (μCP), micromolding in capillaries (MIMIC), solvent assisted micromolding (SAMIM), replica molding (RM), and microtransfer molding (μTM) (see Ref. [193] for a thorough review on each of these topics). The purpose of including a section on soft lithography in this review is to focus on recent advances and uses of these techniques for patterning SAMs, and to highlight the functionalities of the assemblies that have been created using these techniques; the majority of our focus will be on microcontact printing techniques.

6.1. Microcontact printing

Microcontact printing (μCP) as a method of patterning SAMs has grown in popularity due to the ease of fabricating the printing tools, relatively high spatial resolution of features produced (line widths of <100 nm [195]), and large printing capacity (up to tens of square centimeters of sub-micron-sized features can be printed in parallel). Microcontact printing is a technique relevant to creating patterned substrates resulting in binary-component SAMs arranged in simple spatial patterns for the purpose of organized attachment of biomolecules or cells, or to use such printed SAMs as sacrificial layers for complex fabrication of nanoscale materials, to name merely a few applications. Using the concept of *positive placement* to transfer adsorbates to a surface, patterning of SAMs by μCP works by the creation of a flexible, polymeric stamp with patterned reliefs (typically fashioned from polydimethylsiloxane, PDMS) and by dipping the stamp in an alkanethiol "ink".
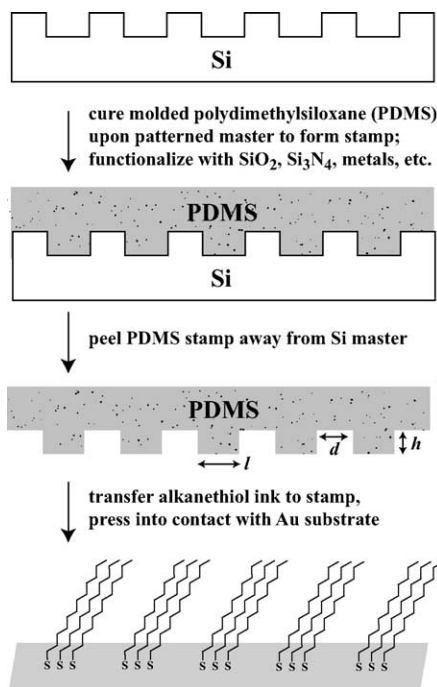
Fig. 20. Schematic of the microcontact printing process, adapted from [193]. The relief patterns of the silicon master are transferred as negatives to the PDMS stamp; the dimensions of post width '*l*', post separation '*d*', and post height '*h*' are critical for proper transfer of molecules and pattern fidelity across multiple transfers.

Once the stamp has been inked and dried, the stamp is then briefly pressed against a gold (or other thiol-compatible) substrate via mechanical contact, and the alkanethiolate molecules transfer from the polymer to the substrate beneath where they self-assemble into patterns pre-determined by the relief patterns of the stamp, Fig. 20 [193]. Binary-component SAMs are then formed by backfilling the non-patterned areas with a different adsorbate. The μCP technique is attractive because it is inherently rapid and can be performed in parallel, for many features can be printed simultaneously with one stamp application. In addition, it is generally cost-effective and can be applied to many substrates and desired patterns. However, the resolution of the resulting patterns is limited by the material and dimensions of the elastomeric stamp. Furthermore, the reproducibility of the process is dependent on the stamp's resistance to degradation, the replication accuracy of the contact pressure that is applied to the substrate, and registration with other surface features. Typical features that have been constructed are on the order of hundreds of nanometers to micrometers, although structures with dimensions as low as 30 nm have been reported [197].

6.2. Elastomer stamp fabrication

The first step in µCP and other soft lithographic techniques is the fabrication of the elastomeric stamp or mold. Generally, the elastomer is cast onto a silicon master that has been patterned and etched by electron beam lithography or photolithography to contain the desired relief structure on its surface, Fig. 20 [194]. The elastomer is then thermally cured and peeled off; this master can be reused for further replication of the elastomeric stamp or mold. Additionally, pre-fabricated, commercially available structures such as transmission electron microscopy grids or diffraction gratings can be used as masters. However, alternate methods of producing templates for stamp fabrication have been demonstrated, those that do not employ lithography to form the relief patterns [198].

It is important to stress that although soft lithography techniques capitalize upon low cost and simplicity, the most common practice to construct the master from which the stamps are formed remains standard lithography, which is typically expensive and time-consuming. Whitesides and coworkers have developed alternative methods to create masters that do not rely on such lithographies; rather, the basic ideas used in soft lithography are implemented in order to produce the masters themselves [198]. For example, masters have been produced by µCP of an *n*-hexadecanethiol SAM onto silver substrates. In this case, the printed SAM is used as an etch resist and the surrounding Ag can be selectively etched away, creating a silver substrate with relief features etched into it. This pattern can then be used to cast additional PDMS stamps for microcontact printing [198]. Other methods using this same general idea (i.e., casting a PDMS stamp from polymers cured on surfaces of Au that have been printed with a hexadecanethiol SAM) have also been demonstrated [198]. While these examples are encouraging steps toward the reduction of photolithographic techniques for the production of master structures, the resolution of the features generated using non-lithographically patterned masks is greatly compromised and typically not less than 1 µm. It will be necessary to improve upon these methods or innovate new methods in order to advance beyond this limitation.

The elastomer that is used in these techniques is most commonly PDMS, although other polymeric materials such as phenolformaldehyde polymer (Novolac resin), polyurethanes, and polyimides have also been used. PDMS is favored because it is a rugged, chemically inert material that can be reused many times. The material cures under moderate conditions (65 °C for 2–24 h, or 100 °C for 1 h) and is easily removed from surfaces, making it amenable to patterning complex structures on delicate or non-planar surfaces [193]. As illustrated in Fig. 20, the dimensions of d, h, and l are of critical importance for pattern transfer. The resolution, reproducibility and stability of features produced using soft lithography are often dictated by the properties of the elastomeric stamp or mold. Therefore, it is crucial that the material properties of the elastomer are appropriate for the desired structure. Challenges associated with using an elastomer such as PDMS include capillary forces that cause the pattern to spread after conformal contact, as well as gravitational or adhesion forces that can cause unintentional contact between the stamp or mold and the substrate. To this end, the conformal and adhesion properties of elastomeric
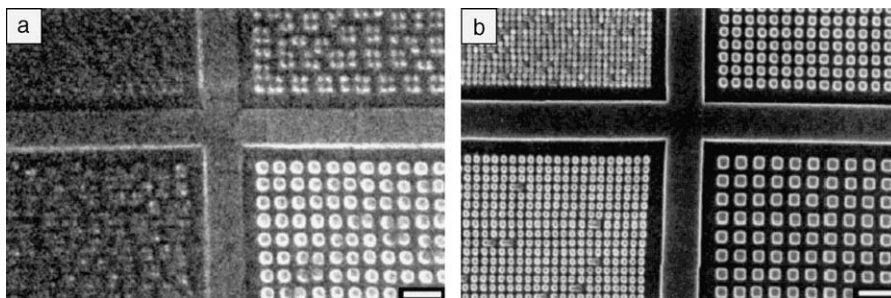
Fig. 21. SEM images showing that the sharpness of features produced by μCP can be increased by changing the composition of the elastomeric stamp. The scale bar corresponds to 1 μm. The image on the left shows features printed using commercially available PDMS, and the image on the right shows features printing using a slightly stiffer (more crosslinked) PDMS-based elastomer. Adapted from Ref. [200], and reproduced with permission of the American Chemical Society.

materials have been extensively investigated [199]. It is important to note that increasing the stiffness of the elastomeric material produces patterns that are more stable and reproducible; however, stiffer materials decrease the conformability of the stamp or mold, thereby reducing the contact between the stamp and the substrate and causing defects in the pattern. In addition, stiffer materials limit the versatility of the patterning technique since these cannot be used with non-planar substrates. Therefore, an acceptable balance must be achieved between the conformability and stiffness of the material in order to produce stable patterns, Fig. 21. Also, fundamental studies have been performed to determine appropriate aspect ratios of d, h, and l in order to maintain proper pattern transfer. At the proper ratio(s) there will be no buckling of the posts when pressed to the substrate, the posts will not be adversely drawn together through capillary action when inked with solvent, and no other such degradation of the stamp will occur.

Michel and coworkers have manipulated the chemical composition of the PDMS elastomer to increase its stiffness somewhat, resulting in sharper feature edges with less of the adverse spreading that occurs as a result of mechanical contact transfer. They have worked toward creating polymers of increasing stiffness by starting with PDMS precursors and adding more crosslinking functional groups; a slightly stiffer polymer improves upon pattern transfer, yet still maintains the physical properties of PDMS (i.e., flexibility, low surface free energy) that make it such a desirable material for a reusable stamp, Fig. 21 [200]. In most cases, the size of the desired feature can help determine the proper hardness of the material, i.e., the smaller the pattern, the more rigid the elastomer [199]. Additionally, certain non-polar solvents can deform the material and cause it to swell during the inking or cleaning processes. These factors all contribute to the final resolution and precision of the pattern and must be considered when using elastomeric stamps or mold.

There have been several studies comparing the quality of a SAM formed by soft lithography techniques with traditional solution- or vapor-deposited SAMs [201–207]. The majority of these studies involves SAMs produced using μCP compared to
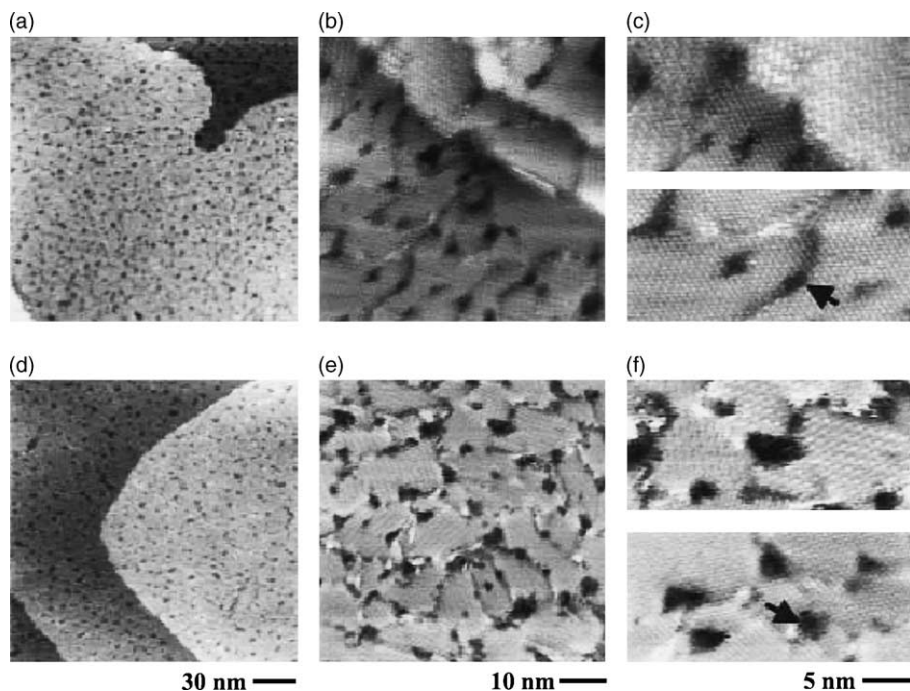
30 nm ——   10 nm ——   5 nm ——

Fig. 22. STM images comparing the quality of alkanethiol SAMs prepared from solution-phase deposition and by microcontact printing. Both SAMs are well-ordered on the nanometer scale, and typical SAM features such as domain boundaries and substrate vacancy islands are seen faithfully across both types of SAMs (arrowheads). STM images A, B, and C are from solution-phase grown SAMs, and images D, E, and F are from SAMs created by μCP. Adapted from Ref. [203], and reproduced with permission of the American Chemical Society.

solution-deposited films studied by a variety of techniques, including scanning probe microscopy [201,203,204,207], IR spectroscopy [201,204], near edge X-ray absorption fine structure spectroscopy (NEXAFS) [202], contact angle measurements [203], scanning electron microscopy (SEM) [205,206], and X-ray diffraction methods [207]. In general, it was shown that the quality of the microcontact-printed SAM is similar to (or better than) that of a solution- or vapor-deposited SAM [204]; however, there are minor disparities between these studies that suggest the order of the system is somewhat dependent on the formation process. Possible dissimilarities between the two processes include differences in packing density [201], tilt angle of the alkyl chains [202], and domain size [207]. Fig. 22 shows that both types of SAMs, those formed from the solution phase and those formed by μCP, are similarly well-ordered at the nanometer scale when imaged with the STM. In addition, the concentration of the inking solution was found to be critical in the resulting order of monolayers formed by μCP. For microcontact-printed alkanethiol SAMs from solutions with concentrations less than 10 mM, it was shown that the printed SAM was relatively disordered and liquid-like, even though the solution-deposited SAMs remained well-

ordered [203]. STM images of microcontact-printed *n*-dodecanethiolate SAMs revealed the familiar $(\sqrt{3} \times \sqrt{3})R30°$ packing structure and that the domain size increased with increasing concentration [203]. Likewise, printed SAMs of octade-cyltrichlorosilane on SiO_2 were more complete at an inking solution concentration of 10 mM, even though solution-formed monolayers were disordered at this concentration [204].

Diffusion processes that occur after the printing process can also compromise the order observed in microcontact-printed SAMs [205,206]. Delamarche et al. described several different diffusion pathways for the molecules in a microcontact-printed SAM [205]. For instance, the inking solution can spread from the surface of the stamp to areas of the substrate not intended for patterning. This process is circumvented by using a dry stamp to allow printing of the vapor-phase molecules trapped in the stamp. There is also the possibility of ink transfer from the stamp to the substrate in non-contacting areas by the vapor phase, which is directly related to the vapor pressure of the inking molecule (i.e., molecules having a high vapor pressure will have a higher chance of this type of diffusion). In addition, the molecules can diffuse along the substrate after the stamping procedure, forming areas of ordered or semi-ordered monolayers. These effects can be reduced by using a lower concentration inking solution, thereby reducing the number of molecules available for diffusion. In order to form a complete monolayer, it is then necessary to increase the printing time (>1 s). Delamarche et al. found that the optimal printing process involves a 0.2 mM solution of eicosanethiol ($CH_3(CH_2)_{19}SH$) printed for 3 s [205]. Obviously, these conditions are not always possible given the desired experiment; however, this study served to demonstrate that it is necessary to find the proper balance between alka-nethiol length, solution concentration, and printing time.

In another study conducted by Libioulle et al., various inking methods were examined to determine the best method for preserving the pattern on the surface [206]. Fig. 23 illustrates the three different methods that were attempted: (1) wet inking, (2) pen-type inking, and (3) contact inking [206]. In wet inking, the PDMS stamp is exposed to a solution of the thiol for patterning such that the entire surface of the stamp is covered with the inking solution. Although this is the easiest method for transferring the inking solution to the stamp, wet inking can be problematic when unintended areas of the stamp come into contact with the surface, causing diffusion of the molecules and broadening of the pattern. This is especially true for when small-scale (<500 nm) patterns are desired. Pen-type inking involves continuous diffusion of the inking solution to the stamp by means of a reservoir connected to the stamp. However, this method did not prove successful because the solvent (in this case, ethanol) swelled the PDMS stamp, producing broadened patterns. In contact inking, the stamp is placed in contact with a PDMS block that has been exposed to a solution of the thiol for 12 h and subsequently dried, thereby acting as an ''inkpad''. Thus, the inking molecules are only transferred to the contact areas of the stamp, drastically limiting diffusion from non-contacting areas. However, the quality of the printed area indicated they were not as well-ordered as in patterns produced by wet-inking since contact-inking relies on diffusion of the molecules from the stamp to the surface. Consequently, this method was demonstrated to be the most effective for
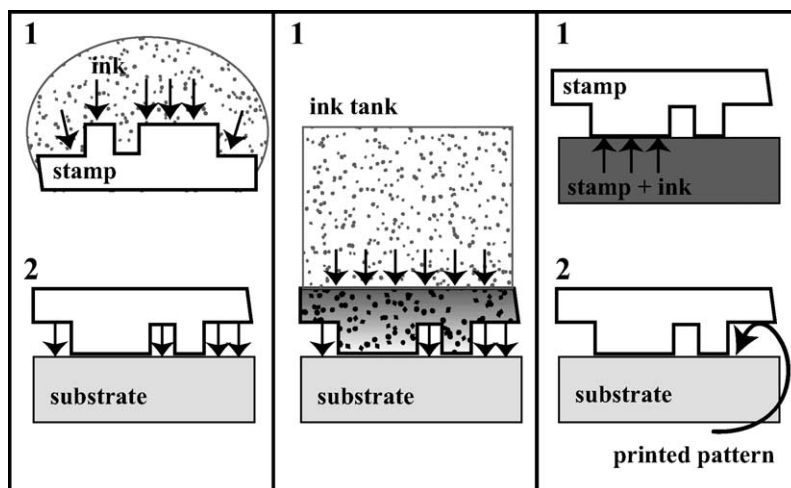
Fig. 23. Three different methods of applying the alkanethiol "ink" to a PDMS stamp. Left panels (1 and 2): wet inking; middle panel: pen-type inking; right panels (1 and 2): contact inking. Taken from Ref. [206], and reproduced with permission of the American Chemical Society.

creating patterns at scales <100 nm when the quality of the printed area is not critical [206].

From these studies, it is evident that the quality of the SAM after soft lithography patterning is dependent on a number of factors, including chemical and physical properties of the inking molecule, concentration of the inking solution, duration of contact, and printing method. In order to produce high-quality SAMs using soft lithography, it is thus necessary to attain a balance between these factors. Often, this can only be achieved empirically, which can make optimizing the patterning method a laborious and time-consuming process. Studies have been performed that have analyzed the degree of contamination in the printing process; for example, Ratner and coworkers discovered through electron spectroscopy for chemical analysis (ESCA) that low molecular weight (uncured) PDMS was being transferred to the substrate during the stamping process along with the thiol of interest; the presence of small yet polymeric molecules could disrupt the local order of microcontact-printed films [208]. To eliminate the problems of contamination, they recommended several cycles of extraction, rinsing, and sonication in order to remove all small fragments of the stamp; they found that the purity of the ordered structures increased as well if the concentration of the inking solution was sufficiently high (10–50 mM).

6.3. Applications using microcontact-printed SAMs

By printing molecules with different terminal functional groups, it is possible to perform chemistry in pre-determined locations. Yan et al. prepared a reactive SAM using μCP that could be used as a patterned surface for tethering both gold and silver

nanoparticles [209,210]. Briefly, a SAM consisting of interchain carboxylic anhydride endgroups was prepared and exposed to a PDMS stamp inked with an amine (*n*-hexadecylamine) [209]. The amines reacted selectively with the anhydride groups that contacted the stamp, producing a SAM containing patterned regions of carboxylic acids and *N*-alkylamides. This mixed SAM was subsequently exposed to a fluorinated amine ($CF_3(CF_2)_6CH_2NH_2$), resulting in a mixed SAM consisting of *N*-hexadecylamides and fluorinated *N*-alkylamides. The edge resolution, measured by scanning electron microscopy and secondary ion mass spectroscopy, was found to be <100 nm. Using this method, it was possible to prepare a mixed SAM containing regions of thiol-terminated and methyl-terminated alkanethiols for the selective adsorption of gold nanoparticles [210]. This method has also been demonstrated as a way to pattern SAMs with polar and charged terminal groups [210,211].

Multicomponent SAMs patterned by μCP can then be used as templates for the selective deposition of other nanoscale materials. Hammond and coworkers have used patterned SAMs as templates for the deposition and selective adsorption of polyelectrolytes in order to create higher order architectures for uses in thin film, organic-based materials. By stamping with a carboxylic acid-terminated thiol and backfilling with an oEG-terminated thiol, it was demonstrated that charged polymers could be selectively oriented on the acidic surface in the patterns predetermined by the stamp [212,213]. Polyelectrolytes of opposite charge (such as
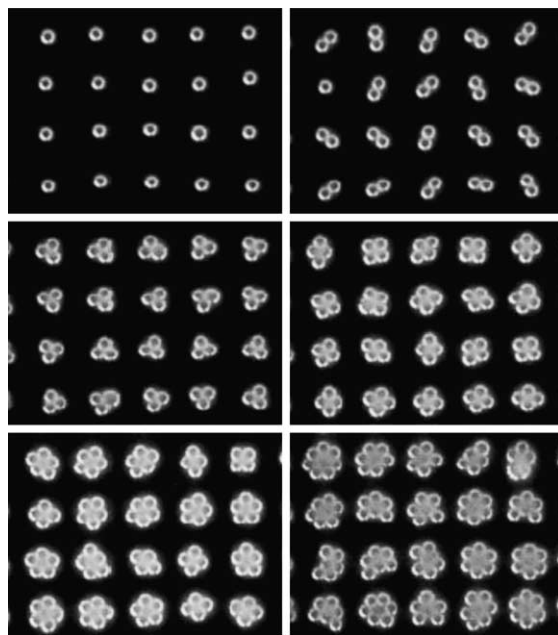

Fig. 24. Assemblies of ~4 μm carboxylated latex colloid deposited on patterned polyelectrolytes. The number of particles aggregating together atop the patterned polymer is controlled by the area of the polymer underneath. Adapted from Ref. [215], and reproduced with permission of Wiley Interscience.

poly(diallyldimethylammonium chloride) and sulfonated polystyrene) could then be stacked, layer by layer, on each other in predetermined orientations. Colloids can then self-assemble on a certain polyelectrolyte area of interest by the specific substrate–colloid interactions [214], and tailored spatial arrangements of colloids can be made by patterning polyelectrolytes in controlled geometries with specific areas [215], Figs. 24 and 25.

This idea can be used to direct the fabrication of inorganic materials. Using μCP, Aizenberg and coworkers demonstrated the growth of oriented calcium carbonate crystals on ω-terminated alkanethiolate SAMs [217–219]. The nucleation of oriented crystals worked most effectively on SAMs that were terminated with acidic funtionalities including $-CO_2^-$, $-PO_3^-$, $-SO_3^-$, and $-OH$, while alkanethiolates that were either CH_3-terminated or slightly basic ($-N(CH_3)_3^+$) inhibited crystal growth. Periodic arrays of oriented crystals can be produced by using μCP as a method of templating substrates. Han et al. have also demonstrated the growth of calcite crystals in a periodic array; after forming a SAM of 4-nitrobenzenethiolate, they irradiated portions of the SAM with a visible laser ($\lambda = 514.5$ nm) through a mask. The molecules in the exposed parts of the SAM were reduced to $-NH_2$ groups, and the calcium carbonate crystals nucleated selectively in these regions [220], Fig. 26.

Properties such as luminescence (for the thin film functionality) can be integrated into the layer by layer assembly process [221]. Overall, factors such as solution ionic
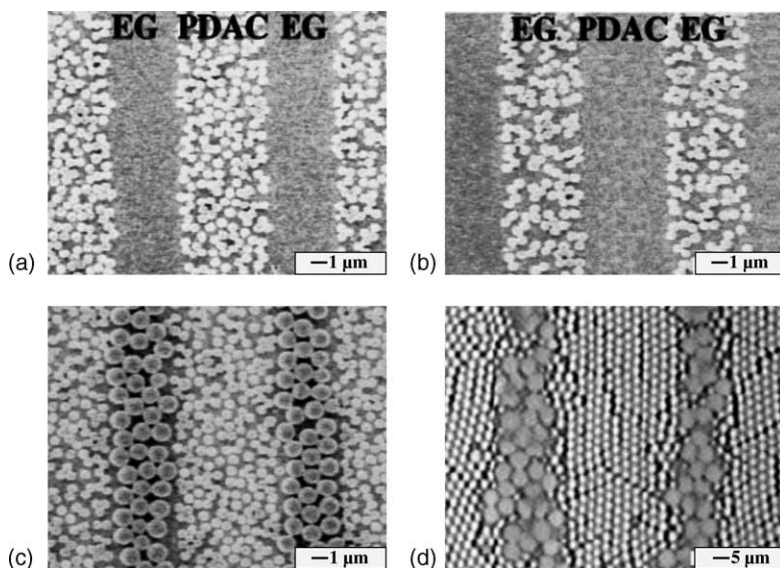
Fig. 25. Assemblies of functionalized latex colloid have been deposited on patterned polyelectrolytes (EG = ethylene glycol-terminated alkanethiol, PDAC = poly(diallyldimethylammonium chloride). It is possible to create patterned arrays of colloid directed by the patterned substrate underneath. Adapted from Ref. [216], and reproduced with permission of Wiley Interscience.
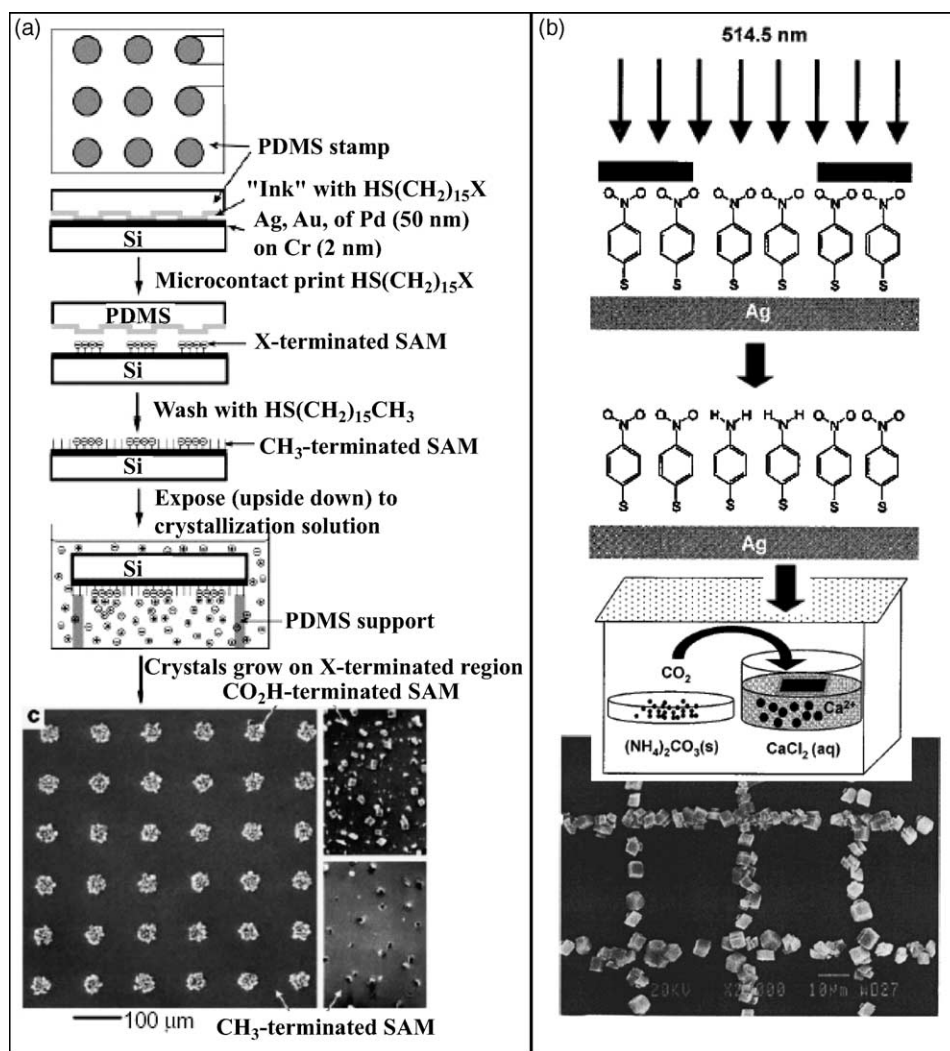
Fig. 26. Schematics of the assembly of ordered arrays of calcium carbonate crystals formed upon SAMs patterned using either soft lithography or photons. (a) A PDMS stamp is inked with a carboxylic acid-terminated alkanethiolate and then backfilled with a non-reactive, methyl-terminated alkanethiol. The calcium carbonate crystals nucleate on the acid-terminated regions in ordered arrays (left figure); crystal nucleation events are spatially random when performed upon homogeneous SAMs (right figures). (b) Regions of a 4-nitrobenzenethiolate SAM were irradiated with visible light through a mesh grid; the –NO$_2$ groups of the exposed portions were reduced to amines, upon which calcite crystals could selectively nucleate. '(A)' was reproduced from Ref. [218] with permission of MacMillan Publishing; '(B)' was adapted from Ref. [220], and was reproduced with permission of the American Chemical Society.

strength, charge shielding phenomena (such as the inclusion of surfactants in the solution) and secondary interactions (i.e., electrostatic attraction or repulsion, van

der Waals forces) can be manipulated in order to control the structure of the final assembly [222].

6.3.1. SAMs as ultra-thin etch resists

The ability of *n*-alkanethiolates to bind to metal surfaces and form well ordered thin films makes them ideal for passivating the surface towards corrosion. This property is of prime utility in lithography techniques, where the surface is greatly reduced to attack by etching/oxidizing solutions. An entire surface can be passivated by a SAM, or areas of a metal surface can be selectively protected against etching by microcontact printing thiol in certain areas; the non-passivated regions would etch at a much faster rate than the non-protected regions. The use of SAMs as etch resists to alkaline CN^-/O_2 solutions (a known oxidant of Au) was reported by Kumar et al. [98,223]; trenches on unprotected regions of the Au were formed, while the regions of SAM-covered Au experienced little disintegration or pitting. A variety of etching conditions were reported later [224]. Similarly, the presence of a SAM atop a gold surface can prevent the electroless deposition of nickel [224].

Whitesides and coworkers have developed the technique of topographically-directed etching (TODE) in which the varying degrees of order in SAMs are used to advantage and function as etch resists or as supports for electroless metallization [219,225]. Generally, a metal is evaporated onto a different metal substrate through a photoresist mask and is exposed to a solution of alkanethiols. The formed SAM is less ordered at the transition region between the two metals and as such, is more labile to exchange with other alkanethiol molecules in solution, directed crystal nucleation, or etching processes, Fig. 27. TODE has been successful in etching ∼100-nm trenches on various substrate systems, including Ag/Ag (top metal/bottom metal), Au/Ag, SiO_2/Si, and Al_2O_3/Al, as well as non-planar Ag surfaces. An additional advantage to this technique is that it is capable of forming both raised and entrenched features.

Microcontact printing has been used to etch Au/Ti layers atop GaAs-based materials; layers of Ti and Au were evaporated atop GaAs/AlGaAs multiquantum well structures, and then were selectively etched away using μCP-printed SAMs to protect particular areas of the surface [226]. The exposed GaAs could then be subsequently etched away, transferring the pattern.

6.4. Nanotransfer printing

The process of nanotransfer printing (nTP) to pattern features on surfaces is an elegant complement to microcontact printing. Whereas μCP aims to print SAMs on surfaces where the configured elements are the alkanethiolate molecules attached to the gold substrate, the concept of nTP is to print metal features atop a SAM-functionalized substrate, where the SAM serves as an adhesion layer between substrate and patterned metal film. Nanotransfer printing aims to increase the edge resolution of patterned metal features further, as this is often a limiting factor. Features printed by μCP are limited in resolution not only by the smearing of edges as a result of the deformation of an elastomeric stamp, but also by the diffusion
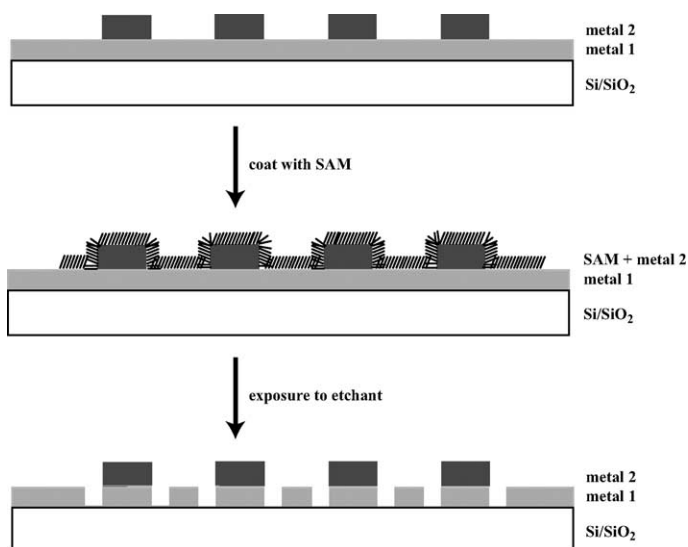
Fig. 27. Scheme of topographically directed etching. Disordered regions of an alkanethiolate SAM (here, adsorbed on a patterned metal substrate, where metal 2 has been evaporated atop metal 1) are susceptible to preferential etching. Trenches result alongside raised features. Adapted from Ref. [225], and reproduced with permission of the American Chemical Society.

(albeit limited) of alkanethiolate adsorbates. Nanotransfer printing experiments have been performed using a variety of materials for substrates and stamps; well-defined surface chemistry is required in order to build up to the complex patterned features. The edge resolution of the patterned features is between 5 and 15 nm, which is comparable to the edge resolution of the PDMS stamp itself as well as the grain size of the evaporated gold metal. Fig. 28 demonstrates the types of features that can be patterned upon both firm and flexible substrates.

7. Patterning SAMs with energetic beams

While soft lithography has moved the field of patterning SAMs forward at an enormous rate, the field of using energetic beams to pattern SAMs has also advanced considerably. Self-assembled monolayers and multilayers have been used to assist in bridging the nanofabrication gap in the critical 10–100 nm range that is currently difficult to achieve by current lithographic methods [181,228]. Energetic beams such as ions, electrons, and photons are routinely used to destroy polymer resists, and etch into other structures. However, the effectiveness of polymer resists is limited by their thickness. SAMs, both of organothiols on gold as well as organosilanes on silicon surfaces, have assisted in advancing conventional lithography by serving as sacrificial resists (i.e., chemically modifying the SAM so that different regions will
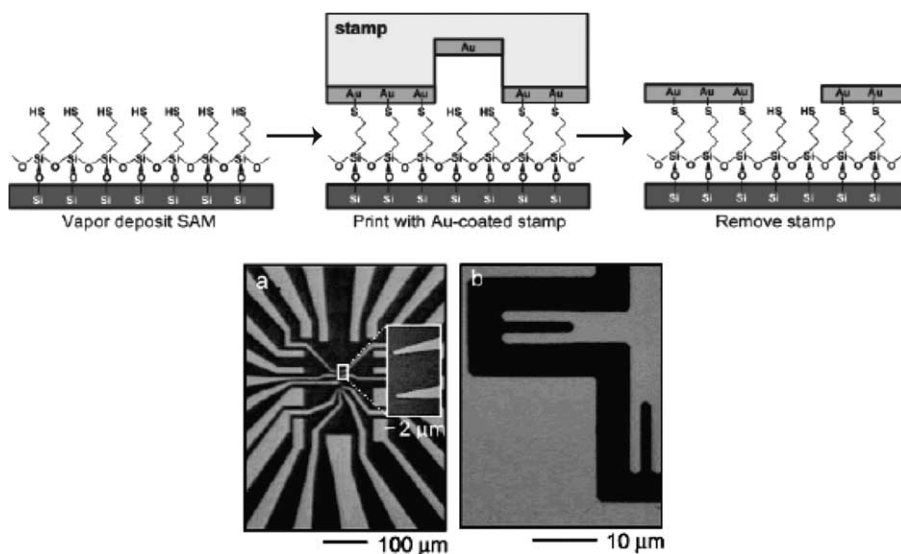
Fig. 28. Top: Scheme of the nTP process. A thiol-terminated SAM is formed on the native oxide of a silicon substrate, and a PDMS stamp with a thin layer of evaporated gold upon it is briefly contacted with the substrate. Removal of the stamp leaves Au metal only in the patterned areas. Bottom: Optical micrographs of Au patterns on two types of substrates created by nTP. (a) A Au pattern printed on a silicon wafer. (b) A Au pattern printed on a flexible poly(ethylene terephthalate) substrate. Reproduced from Ref. [227], and with permission of the American Chemical Society.

vary in their susceptibility to attack by wet etches) [229,230]. For using SAMs as etch resists, one can either destroy the SAM in a patterned fashion via energetic beams, or one can pattern by μCP, leaving bare areas (*vide supra*).

Although inorganic resists are widely used in lithographic applications, there are several drawbacks that make ultra-thin organic materials such as SAMs attractive alternatives to conventional resists. For instance, inorganic resists require high electron beam dosages, as the mechanism for their destruction is based on damage to the material by the electron beam. In addition, high energy electrons are also needed to permeate thick layers of material, yet they can cause a cascade of backscattered electrons that damage the surrounding areas, hence broadening the features [231]. Some of the earliest work on using SAMs as electron beam resists was using SAMs of alkanethiolates on GaAs [86,232], and SAMs of octadecyltrichlorosilane (OTS) on SiO_2 [233]. These SAMs serve as positive, self-developing resists, as they degrade upon exposure to the electron beam; wet chemical etching in the exposed regions leads to features entrenched in the substrate. AFM imaging confirmed the degradation of the SAMs upon exposure to the electron beam and before chemical etching, indicating their exposure [86]. Isotropy of etching is most often impossible at the nanometer scale. Here in the SiO_2 work, SAMs are used as electron cyclotron resonance–reactive ion etching (ECR–RIE) masks; this has also been shown to work for thiols on GaAs and OTS on Ti.

The pattern transferred to the SAM is a function of the mask that is placed in the path of the beam and the sample. Grunze and coworkers have adsorbed 4′-nitro-1, 1′-biphenyl-4-thiol (NBT) on a gold surface and then irradiated the sample with 50 eV electrons through a copper transmission electron microscope grid (a pattern of squares, 20 μm per side) [234]. The NBT molecules form an ordered SAM as shown by IR, XPS, and NEXAFS [235]. The exposed nitro groups are reduced to amino groups, and the chemical bonds of the underlying aromatic layer break and crosslink to those of nearest neighboring molecules (these chemical events were confirmed by IR and XPS) [234]. A non-irradiated SAM was exposed to *n*-dodecanethiol, which completely displaced all of the NBT; after the SAM was exposed to radiation, the alkanethiol was not capable of displacing it. Also, the irradiated SAM was impervious to KCN etching solution (a known etchant of gold), making the irradiated SAM serve as a negative resist, as shown in Fig. 29. They demonstrated that the chemical species of the irradiated monolayer were amine groups by reacting the pendant terminal with trifluoroacetic acid anhydride, rendering the $-NH_2$ groups $-CF_3$ terminated. Imaging with LFM showed the differing areas of friction, with the very hydrophobic $-CF_3$ imaging as regions of low lateral force versus hydrophilic $-NO_2$ groups, imaging as regions of high lateral force [234]. Geyer et al. also immobilized rhodamine dyes to the terminal amine groups, and with laser scanning confocal fluorescence microscopy and LFM demonstrated the presence of amine groups [236].

This ultra-thin resist system is successful both because of the thinness of the resist and the low mean free path of the low-energy electrons. Also, even at high doses of ∼50 eV electrons, the SAM is not destroyed. The irradiation of the NBT molecule gave a minimum feature line width of 20 nm [236–238].
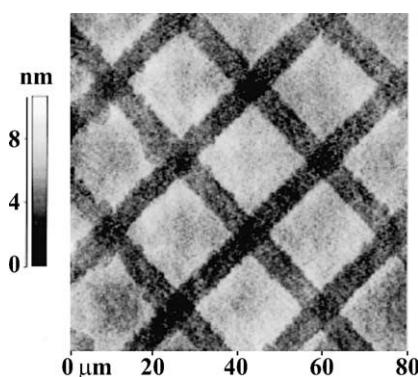
Fig. 29. AFM image of an arylthiolate SAM atop a Au substrate, followed by exposure to 10,000 μC/cm^2 of 50 eV electrons through a mask and subsequent exposure of the irradiated sample to a wet etch of 0.2 M KCN/1 M KOH. The non-irradiated portions of the SAM are selectively etched away (dark, topographically lower), while the crosslinked resist protects the underlying Au substrate. Adapted from Ref. [235], and reproduced with permission of the American Institute of Physics.

Gold nanostructures have been fabricated using positive- and negative-tone resists (*n*-alkanethiolate and arylthiolate SAMs, respectively) [239]. Weimann et al. claim that the resolution of electron beam lithography in etching away resists is the size of the molecules in the resist. They use aliphatic SAMs as positive-tone resists, as the radiation beam induces damage and disorder of the chains (Au–S bond cleavage, irregular crosslinking, etc.); they use arylthiolate SAMs as negative-tone resists, as the organic layer is strengthened by crosslinking rigid aromatic units (similar to the work by C–H bond cleavage by radiation, followed by crosslinking). Using a scanning transmission electron microscope as an ultra-sharp source of electrons, they have achieved features that have minimum linewidths of 20 nm (for both types of SAMs). Pattern transfer and anisotropic etching are the limitations in these studies; electron beam energies used were 200 keV and 2.5 keV, depending on the substrate [239].

Grunze and coworkers have also performed studies on the irradiation of *n*-alkanethiolate SAMs for use as positive-tone resists; they examine the fundamental chemistries that occur to the SAM as a function of beam irradiation in order to improve its use as a resist [240]. The most noticeable processes that occur with damage are the loss of the SAM's orientational and conformational order, partial dehydrogenation with C=C double bond formation, desorption of the layer fragments resulting in reduced film thicknesses, and reduction of the thiolate species as shown by the appearance of new sulfur species. The longer the length of the alkyl chain, the slower the desorption of the thiolates. Whereas the irradiation-induced processes in the alkyl matrix are found to be essentially independent of the alkyl chain length and the substrate material, the extent and rate of the thiolate species reduction and new sulfur species formation are mainly determined by the strength and character of the thiolate–substrate bond. They studied *n*-dodecanethiol, *n*-octadecanethiol (ODT), and perdeuterated eicosanethiol on Au, and ODT on Ag. The isotopic effect was shown to be minimal, barely slowing the rate of molecular conversion [240]. They note that the damage to SAMs caused by ionizing, energetic beams is related to low-energy secondary electrons arising as a result of the inelastic scattering of the primary electrons created within the photoemission process [241]. The damage to the film by the incident electron beam causes the desorption, breakdown, and chemical rearrangement of the molecules, yielding a film of new molecular composition.

Craighead and coworkers have performed low energy electron beam studies of NH_2-terminated organosilane SAMs on SiO_2, irradiating with <5 keV energy so that the primary damage of the SAM occurs at the terminal amine group [242]. They found that the lower the energy of the electron beam, the higher the resolution of the feature; with the beam at low accelerating voltages, most of the energy is left in the top part of the SAM and the terminus is selectively damaged. The goal of their studies was to produce patterned *amine*-functionalized SAMs whereupon radiation with the electron beam, the amino groups are destroyed. One can then pattern the unexposed, remaining –NH_2 groups; they demonstrated the selective adherence of palladium nanoparticles, aldehyde-functionalized polystyrene spheres, and Neutr-Avidin-coated polystyrene spheres [242]. They demonstrated several schemes to

pattern amine-terminated SAMs, i.e., irradiating a methyl-terminated SAM with low energy electrons followed by backfilling the destroyed regions with cysteamine generated phase-separated SAMs, with the binary component SAM presenting both CH_3- and NH_2- termini [243]. They reacted the terminal amines in the phase-separated domains so as to present biotin moieties that would selectively react with NeutrAvidin-coated polystyrene spheres. By varying the electron dosages, molecular gradients could be generated. Bard et al. exposed alkanethiolate SAMs to meta-stable, excited noble gas atoms (both helium and argon atoms) in order to damage the resist; after the damage, the gold substrates were exposed to wet chemical etches and the patterns were examined by AFM and the reflectivity of the substrate was measured [244]. This 'neutral atom lithography' is highly beneficial in the fact that neutral atoms have an extremely short de Broglie wavelength (<0.1 nm) unlike their photon counterparts, and they only interact with the outermost layer of a surface (concentrated damage with no further penetration), unlike other species, which can scatter and broaden a feature on contact with the surface.

Organosilane SAMs have also been patterned with electron beams; the silicon was then etched with HF, and nickel was electroplated atop the exposed silicon (nickel is an excellent mask for RIE processing) [233]. Additionally, one can pattern an organosilane SAM with photons ($\lambda = 157$ nm) via a photomask [245]. Sugimura et al. demonstrated that they could electrolessly plate nickel in the exposed regions, followed by an additional etch with a plasma in the exposed regions. Low energy electrons ($\sim$500 eV) have also been used to pattern trimethylsilyl SAMs. The irradiated regions were destroyed in striped patterns, and an amine-terminated silane was backfilled in those regions [246]. Bundles of single-wall carbon nanotubes could be selectively deposited in the positively charged striped patterns.

8. Scanning probe-based lithography

Patterning of surfaces with scanning probe microscopes such as the AFM and the STM has been explored, as the location of the probe tip can be placed on the surface at a specific set of coordinates and the resolution of the patterns can approach the molecular scale. Changing the location of the probe tip on the surface allows the ability to ''write'' patterns into a surface; typically, changes in the surface that have been effected are either the direct placement of molecules, probe-tip mediated replacement or desorption of surface-bound molecules, or probe tip-catalyzed surface reactions, thus changing the chemical properties of the interface. Additionally, utilizing local probes to create patterns is especially exciting as the probes are capable of both creating the pattern as well as characterizing its structure and placement both before and after the process. Schematics of the various types of scanning probe lithography (SPL) are shown in Fig. 2. Unfortunately, the speed at which these serial processes are accomplished is often slow, and many efforts are now being made towards making the patterning and assembly processes more parallel through the integration of multiple scanning probe tips [247,248].

8.1. Patterning with the atomic force microscope

8.1.1. Dip-pen nanolithography

Dip-pen nanolithography (DPN) is a variety of scanning probe lithography ("direct-write") developed by Mirkin and coworkers, where molecules are transferred by means of an AFM tip to a substrate [123]. As the scanning probe tip can be positioned or programmed to move in certain patterns, it is possible to use DPN to pattern SAMs with different molecular components; these patterns can then be used for the further design of nanoscale structures, by either selective molecular reaction or deposition in the patterned areas.

In particular, they have used *n*-alkanethiol molecules (and their derivatives) suspended in droplets at the end of an AFM tip as a molecular ink. By rastering the probe tip close to a gold (or other metal) surface, the alkanethiol molecules are transported to the surface via capillary action through a water meniscus that naturally occurs between the tip and sample in ambient conditions. An array of molecules are deposited that is a direct function of the rastering pattern of the AFM tip. Dip-pen resolution is down to linewidths of ~15 nm, a result that is a complicated mixture of factors including relative humidity, scan speed, and the relative solubility of the molecule in the water meniscus (different molecules will have different transport rates through this meniscus). It is then possible to backfill the bare regions with other thiol-functionalized molecules simply by exposing the patterned substrate to a thiol solution, and these adsorbates backfill the bare regions. Further studies of the transfer process have led to the DPN-printing of several molecules and novel materials, from alkanethiols to oligonucleotides to sol–gel precursors that afford mesoporous films upon processing after deposition. Also, periodic arrays of nanoparticles have been assembled by patterning thiol-modified oligonucleotides on a gold substrate and then exposing the substrate to a solution of nanoparticles that have been functionalized with the complementary oligonucleotide.

The concept of DPN is that the positive printing of molecules is directly analogous to writing [123]. By holding the thiol-laden AFM tip in contact with a gold substrate for varying amounts of time either by allowing the tip to dwell in a certain location at a fixed distance from the substrate or simply by rastering the tip at a particular speed, it is possible to pattern different size features (i.e., dots, lines) by allowing molecules to diffuse down to the substrate, Fig. 30.

The S–Au bond affixes the molecules to the substrate, and thus their diffusion is limited by the enthalpic forces holding the assembly together (van der Waals between the chains, known as "autophobic pinning" [249]). Molecules with different chemical functionalities pattern somewhat differently. For example, 16-mercaptohexadecanoic acid transfers more quickly to the substrate than *n*-octadecanethiol, as the spots are larger when transferred to the substrate for fractions of the time (minutes as opposed to seconds, an effect of the comparatively higher solubility of the acid-functionalized molecule in the water meniscus and/or crystallization of the molecule upon the surface of the tip). Factors such as tip-substrate contact time, scan speed, and relative humidity all affect the resolution of patterned features. Lateral force micro-
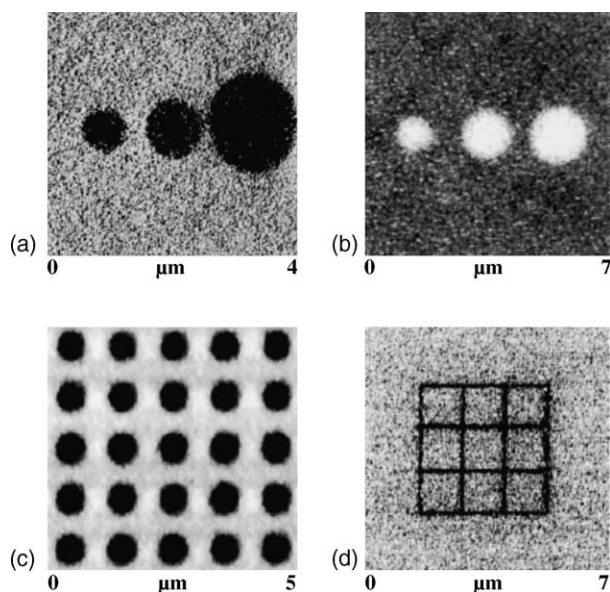
Fig. 30. Lateral force microscope images of thiol molecules printed on Au substrates using DPN. (a) The AFM tip, here coated with ODT, had been in contact with the substrate for 2, 4, and 16 min (left to right); the relative humidity was held constant at 45%. (b) The AFM tip, here coated with 16-mercaptohexadecanoic acid, was held on the Au substrate for 10, 20, and 40 s (left to right); the relative humidity was 35%. The images show that the transport properties of 16-mercaptohexadecanoic acid and of ODT differ substantially. (c) An array of dots generated by holding an ODT-coated tip in contact with the surface for 20 s. Writing and recording conditions were the same as in (a). (d) An ODT molecule-based grid. Each line is 100 nm in width and 2 mm in length and required 1.5 min to write. Reproduced from Ref. [123], with permission of Science.

scopy, in which the AFM measures the relative frictional properties of adsorbates, is used to image the different molecules patterned on the surface.

Dip-pen nanolithography is amenable to printing molecules with a variety of functional groups, as the chemistry of self-assembly has been so well studied and the physical properties of the monolayers so thoroughly investigated that many materials can be patterned using DPN-printed substrates as supports for increasingly complex structures. Generally, the SAMs of alkanethiols that form via DPN will be well ordered, with the sulfur headgroup attached to the Au interface, and with the tailgroup of interest presented at the film–air interface. The self-assembled structures that are printed can be used with confidence, although much effort has been devoted to elucidating the true mechanism behind DPN-based patterning. For example, De Yereo and coworkers purport that the most critical factor in the patterning of alkanethiol molecules onto gold substrates using an AFM tip is the detachment of the thiol from the Si_3N_4 tip, where a bulk precipitate of the thiol molecules has formed as a result of their limited solubility in the water meniscus (yet it is through this meniscus that they are transported) [250]. They have examined the activation energy

of the thiol's detachment from the tip and refined the transfer mechanism through the analysis of factors such as tip scan speed and relative humidity.

Dip-pen nanolithography has been developed for numerous applications, and with multiple substrate materials. For example, DPN has been used to pattern thiols on gold substrates where the partial SAMs were utilized as etch resists (similar to studies in which SAMs were patterned by microcontact printing) [251]. Gold films were evaporated atop silicon substrates, and thiols were printed on the substrates by DPN. The assembly was exposed to wet chemical etches to remove the Au and Ti adhesion layer, along with the underlying Si substrate; three-dimensional nano-structures with anisotropic features as well as those with isotropic features (pillars) were produced by this technique.

Dip-pen nanolithography has also been used to pattern arrays of larger particles, including nanoparticles, proteins, cells, and precursors for mesoporous, inorganic films. Nanoparticles have been patterned on SAM substrates by a variety of methods using DPN. Periodic arrays of differently sized nanoparticles have been anchored to surfaces by patterning oligonucleotides on gold substrates and then exposing the surface to a solution of nanoparticles whose surfaces were functionalized with the complementary nucleic acid sequence [252]. In this work, Mirkin and coworkers demonstrated that multiple particles can be selectively patterned by marking one area of the substrate with a particular oligonucleotide, shifting the registry of the AFM tip pattern, and printing a second oligonucleotide pattern. Exposing the pattern to a solution of nanoparticles that are specifically functionalized to adhere to their particular regions results in selective patterning of the nanoparticles; this was verified by fluorescence microscopy of labeled DNA as well as by tapping mode AFM imaging of the particles, Fig. 31. In this study, thiol-functionalized oligo-nucleotides were patterned on gold substrates, and acrylamide-functionalized oligo-nucleotides were patterned on SiO_2 surfaces derivatized with pendant thiol groups.

Arrays of citrate-stabilized nanoparticles have been patterned by first depositing dots of 16-mercaptohexadecanoic acid (MHDA) in a diluent of a methyl-terminated thiol (n-octadecanethiol, ODT), followed by attaching amine-terminated DNA to the MHDA dots followed by exposing DNA-tagged surface to nanoparticles that have been modified with the complement [253]. The optical properties and function (i.e., catalysis, photonics) of a periodic array of nanoparticles can be changed by altering the composition of the particles; Demers et al. have also patterned posi-tively-charged dielectric spheres by patterning MHDA (in a diluent of ODT) and then adsorbing amine- and amidine-modified polystyrene (PS) spheres. Electrostatic forces drive the assembly, and the degree of assembly could be controlled by changing the chemical environment (charge) of either the surface or the spheres [254].

Thus far, most DPN work has been done with the model alkanethiolate–Au system, where the molecular inks used have included n-alkanethiols, arylthiols, and thiol-functionalized proteins and alkanethiol-modified oligonucleotides for Au substrates. However, alkylsilazanes and inorganic salts for oxidized Si surfaces, and alkylsilazanes for oxidized GaAs have also been investigated. Not merely limited to printing organic materials, Mirkin and coworkers have recently demonstrated the
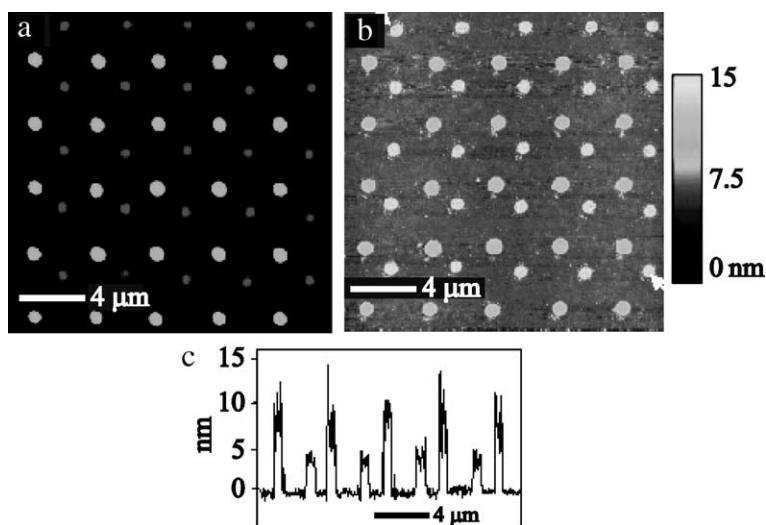
Fig. 31. (a) Two-color fluorescence image of two differing, periodic arrays of oligonucleotides patterned with DPN, followed by hybridization of fluorescently labeled complementary nucleic acid sequences. (b) AFM image of two sizes of nanoparticles (13 and 5 nm) that are functionalized with the complementary oligonucleotides to those patterned with DPN, where each nanoparticle is designed to target either one patterned nucleotide sequence or the other. (c) Line scan through both sets of particles, showing the specificity of the interactions. Adapted from Ref. [252], and reproduced with permission of Science.

patterning of solid-state nanostructures with DPN, i.e., using the water meniscus of the AFM tip to transfer metal ion precursors for the formation of mesoporous thin films [255]. They have shown the ability to pattern inorganic nanostructures by delivering the metal precursors (for the reaction $2MCl(n) + nH_2O \rightarrow M_2O(n) + 2nHCl$), along with a copolymer surfactant that disperses the inorganic "ink" and increases its fluidity and to also make the final structure mesoporous. They have patterned mesoporous films of Al_2O_3, SiO_2, and SnO_2 on Si and SiO_2 surfaces.

In addition to patterning nucleic acids, Mirkin and coworkers have patterned proteins with DPN, resulting in 100–350 nm features [256]. After printing MHDA and backfilling with an oEG-terminated alkanethiol, they demonstrated that proteins would adhere selectively in the acid-terminated regions and that there was no adventitious sticking of proteins (even in a solution containing multiple proteins) to the oEG-terminated regions. They demonstrated control of the height of the arrays by controlling the shape of the proteins patterned. Patterning of lysozyme, an ellipsoidal protein, gives an array height of 1–2 layers of protein, while patterning of Immunoglobulin G (IgG, Y-shaped) gives an array height only ~1 protein molecule thick. Anti-IgG was also exposed to a substrate where IgG had been patterned on MHDA; anti-IgG adsorbed to the IgG-patterned regions. Similarly, experiments were conducted where Retronectin, a recombinant fibronectin fragment containing cell-binding domains, was patterned on MHDA regions; after exposing the substrate to fibroblast cells, it was shown that the cells were selectively located in the

Retronectin regions, after which they demonstrated confluence by flattening and spreading.

Cowpea mosaic virus particles have also been patterned using DPN, where molecules with maleimide termini were printed on a gold substrate [257]. As maleimide groups are highly reactive to thiol groups, mutant virus particles engineered to possess cysteine residues all over their surfaces were exposed to those regions, immobilizing selectively.

Mirkin and coworkers have also patterned magnetic particles via DPN, demonstrating that both inorganic and organic materials can be patterned with DPN [258]. They patterned MHDA on a Au substrate and then dipped an AFM tip in a solution of magnetite (Fe_3O_4) particles. They passivated the surface of the magnetite nanoparticles with a cationic surfactant that would help drive the assembly together via electrostatic interactions.

Mirkin and coworkers have used electrochemistry to reduce the feature sizes of dots patterned by DPN [259]. As discussed earlier, applying a reductive potential to the gold substrate causes patterned features to become increasingly smaller; the desorption begins at the feature peripheries and closes inward radially. The authors found that a minimum potential of −750 mV vs. Ag/AgCl was necessary to begin reducing the features; the rate of desorption of the alkanethiolates increased as the potential became increasingly negative.

8.1.2. Using AFM to mediate chemical reactions

McDonald and coworkers have recently reported site-specific catalysis mediated by palladium-coated AFM tips. Palladium is well known for catalyzing hydrogenation reactions in organic chemistry; by coating an AFM tip with Pd metal, the authors were able to catalyze the reduction of terminal azide and carbamate groups on a SAM to fully reduced amine groups by closely approaching a Pd-coated tip to the surface in the presence of a reducing solution [260]. They demonstrated the success of their reactions by then exposing the SAMs with amine-specific reagents.

8.1.3. Replacement lithography

Liu and coworkers have used both AFM and STM to desorb molecules selectively within an alkanethiolate matrix. However, the desorption mechanism differs between the two instruments, Fig. 2; the basis of molecule removal with an AFM is that the molecules will detach from the surface under an increased load force that is significantly greater than the relatively non-perturbative load required for imaging the SAM. The desorption mechanism using STM is electrochemical, in which molecules can be desorbed by sending high energy electrons into the film (i.e., with bias voltages in the range of 3–4 V).

Similar experiments have been performed by Uosaki and coworkers using a current sensing AFM (CS-AFM), where alkanethiolate SAMs are patterned by the selective removal of adsorbates by the application of a positive bias from the tip to the sample [261,262]. Tunneling spectra acquired over both patterned and non-patterned domains of the SAMs yielded resistances that were consistent with previous measurements of the tunneling coefficient β measured by independent

methods, indicating that the features imaged by the CS-AFM were in fact alkan-ethiolate SAMs.

This type of scanning probe lithography is not specific just to systems of *n*-alkanethiolate SAMs on gold; Sugimura et al. have performed similar experiments using organosilane SAMs assembled on silicon surfaces as resists for SPL experiments [263,264]. Using a CS-AFM, lines were drawn into the SAMs, and then the patterned substrates were exposed to an ammonium fluoride and peroxide etch, which isotropically etches into the silicon underneath the SAM that has been electrochemically destroyed in the tip-sample junction. Grooves etched into the Si were optimal with relatively slow patterning speeds (allowing time for the oxidation of the silicon substrate and destruction of the SAM), as well as increased currents and high bias voltages between the tip and samples. Additionally, they have demonstrated that upon exposing the patterned and etched Si substrate to a gold plating solution, Au can be deposited selectively in the regions where the SAM has been removed, and the rest of the SAM-covered substrate remains featureless and unperturbed [265]. Upon oxidation of the silicon substrate electrochemically with the tip, they were able to backfill the regions of destroyed SAM with an organosilane of differing chemical functionality (removing a methyl-terminated silane and replacing it with an amine-terminated silane) [266]. They were able to demonstrate the immobilization of aldehyde-functionalized polystyrene spheres.

Sagiv and coworkers have used "constructive nanolithography" to pattern silicon substrates and the assemblies on them by oxidizing the terminal groups of the molecules with current from a CS-AFM tip, and then reacting the termini with new alkylsiloxane molecules [267]. A patterned surface results, with linewidths on the order of $\sim$10 nm. The patterning is non-destructive, and from these site-selectively reactive surfaces, organic, metal, and semiconductor components can be selectively deposited [268]. They have also created spatially distributed silver islands by coating the top of a thiolate-terminated SAM with silver ions, and then applying pulses from their conductive AFM tip to reduce the Ag^+ ions locally to form islands [269]. Sagiv and coworkers have also combined this constructive nanolithography with surface self-assembly to create nanoparticles and nanowires connected to addressable electrodes [270].

8.1.4. Nanografting

The process of nanografting has been developed by Liu and coworkers as a method for creating both positive and negative patterns in a SAM [124,271]. Using AFM, molecules from a pre-existing SAM matrix are removed by scanning at a force greater than the threshold displacement force. New alkanethiols can then be back-filled from the contacting solution and are "grafted" into the bare areas. By using longer-chain alkanethiols as the grafting solution, a positive pattern can be made; conversely, using shorter-chain alkanethiols produces a negative pattern. In addition, alkanethiols possessing different functional groups (e.g., hydrophilic) can be nanografted, thereby creating a patterned SAM with varying degrees of reactivity which can be used in further applications.

Chen et al. have reported the direct placement of OPE-functionalized thiol molecules within a pre-formed alkanethiolate host matrix via scanning probe lithography, Fig. 32 [272]. Using a STM tip, they applied ~2–4 V pulses between the tip and a dodecanethiolate SAM; they then promptly backfilled with the OPE-functionalized molecules, thus creating a deliberately placed array of 'wire'-type molecules within a relatively insulating host.

8.2. Patterning with the scanning tunneling microscope

Features were also transferred into SAMs of alkanethiolates on GaAs substrates with the STM [273]. The energies used in this system are very low (~10 eV), as the emission of secondary electrons would therefore be expected to be extremely low, and the energies of the tunneling electrons injected into the features are of sufficient energies to break the chemical bonds of the SAM resist. Lines with widths as narrow as 15 nm were produced with the STM.

Gorman and coworkers have examined the process of scanning probe-based lithography of self-assembled monolayers using an STM under fluid media. In addition to performing fundamental studies in order to elucidate the mechanism of STM-based patterning by using methyl-terminated alkanethiolate adsorbates that differ merely in the length of their alkyl chains [274], their goal has been to pattern electroactive molecules specifically (either ferrocene-terminated or galvinol-terminated within a non-electroactive diluent) [275]. Patterned SAMs were formed by depositing methyl-terminated alkanethiols on a gold substrate followed by their partial desorption by rastering an STM tip over the sample in a particular pattern (in ~10–15 nm widths) and at tunneling conditions designed to desorb the molecules. This replacement lithography was performed with the sample immersed in a non-
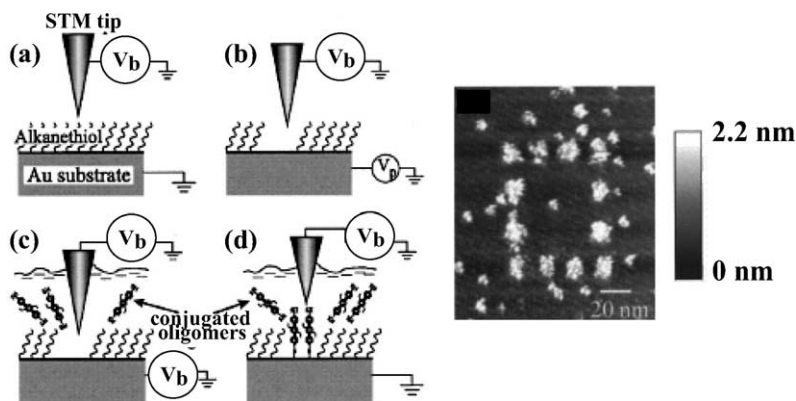
Fig. 32. STM image of OPE-functionalized 'wire' molecules that have been placed into an *n*-dodecanethiolate SAM matrix via reductive desorption of selected regions by pulses with the STM tip, and followed by backfilling the bare regions of substrate with the more conductive molecules. Pulsing conditions: $V_{sample} = 0.1$ V, $i_t = 0.5$ nA, pulse duration = 0.05 µs to 0.5 s. Adapted from Ref. [272], and reproduced with permission of the American Institute of Physics.

polar solvent (dodecane). Electroactive molecules were then backfilled in the bare regions.

They have also reported that by changing the bias voltage while rastering the STM tip across the sample when attempting to desorb adsorbates from the SAM, they are able to vary the linewidths of features. Upon backfilling with a second adsorbate, STM images show that they have created patterns in which the linewidths change in a linear, "gradient-style" fashion [276].

Kleineberg et al. performed scanning probe lithography experiments for systems such as alkanethiolates on gold, arylthiolates on gold, and OTS on SiO$_2$ using STM under ultra-high vacuum conditions [277]. They varied STM parameters such as bias voltage, tunneling current, scan speed, and orientation to carve into the SAM, selectively desorbing molecules in the region of the probe tip. Patterns were then transferred into the underlying substrate by wet etching techniques.

Scanning probe lithography has demonstrated its utility with regard to patterning stable nanostructures followed by the creation of more complex architecture by the selective attachment of new adsorbates, biomolecules, antibodies, or thin films based on the site-directed chemistry enabled by DPN printing. The largest limitation is the slow and serial nature of these processes, such as DPN and replacement lithographies; efforts are underway to enable parallel processing. For example, an array of multiple scanning probe tips for the deposition of thiols has been developed in order to increase the number of features simultaneously patterned [248]. As the feature size patterned is independent of contact force, one can put several tips on one cantilever and pattern the same feature reproducibly [247,248]. Additionally, efforts have been made to interface computer-assisted design (CAD) software with scanning probe microscopes in order to enhance the efficiency of rastering the scanning probe tips in a predetermined pattern [278].

Energetic beams may replace photons for the generation of sub-100 nanometer features and structures; the diffraction of light is the key limiting factor, even with the assistance of phase-shifting masks. However, nanometer-scale patterns have been etched into SAMs by coupling ultra-violet (UV) light with a near field scanning optical microscope (NSOM) [279]. The energy of the UV light destroys selected portions of the SAM in the junction defined by the probe tip, oxidizing the thiol headgroup to a sulfonate; the oxidized products are easily displaced by incident thiols. In this study, portions of a SAM composed of 11-mercaptoundecanoic acid (or of 11-mercaptoundecanol) were selectively irradiated, and then backfilled with *n*-dodecanethiolate. LFM was used to differentiate between the two terminal groups, with the acid and alcohol terminal groups exerting high lateral forces upon the probe tip and the methyl-terminated adsorbates exerting much less. Lines with dimensions as low as ∼40 nm were produced.

9. Patterned self-assembled monolayers in biological applications

The interactions of biomolecules with surfaces are of critical importance to a wide variety of fields, and many self-assembly-based techniques have been employed to

understand these events to the fullest (for excellent reviews of the growing interface between surface science, biology, and bioengineering, refer to [280–282] and references therein). Many of the aforementioned techniques have been used to create novel SAMs in order to create and to investigate the utility of scaffolding and supports for biological applications. Microcontact printing and electrochemistry are two particular methods of patterning SAMs which have found exceptional utility in making SAMs that are selectively activated to study biological events.

Patterning reactive SAMs can also be useful for biochemical and biological purposes. For instance, Lahiri et al. formed a mixed SAM consisting of alkanethiols terminated with an oligo(ethylene glycol) group and a reactive pentafluorophenyl group using standard adsorption procedures [211]. This SAM was brought into contact with a PDMS stamp containing a biotin-containing ligand, which reacted with the activated pentafluorophenyl groups in the regions of contact; the pendant biotin ligands served as points of attachment for streptavidin-functionalized biomolecules. This is a convenient and versatile method to pattern biologically active surfaces and can be useful in biosensors or cell adhesion.

9.1. Patterned self-assembled monolayers to probe cell–substrate and biomolecule–substrate interactions

Microcontact printing technologies have had an enormous impact upon biotechnology studies and experiments. Microcontact printing has been used to fabricate microfluidic arrays in order to create functional devices that require laminar flow or carefully controlled delivery of reagents [283]. For example, μCP has been used to fabricate microfluidic channels that deliver chemotactic agents reproducibly to neutrophil cells in order to study their physical response to gradients of chemoattractants. Microcontact printing has also been used as a technique of patterning cells upon substrates; molecules can be printed in specific locations, resulting in adherence to predetermined regions, followed by their selective release [284].

Mrksich and coworkers have performed elegant studies that control specific interactions between adherent cells and electroactive, self-assembled monolayer substrates. They have used electrochemistry to reduce or to oxidize pendant functional groups at the SAM–solution interface in order to *attach* or to *release* chemical moieties selectively that are important for substrate recognition. They have used simple, well-known biomolecule–protein interactions (i.e., biotin–streptavidin) to demonstrate the proof-of-concept functionality of these ''dynamic SAMs'' and have proceeded to work with more complicated entities such as cells or proteins once the interactions were understood. Mrksich has combined soft lithography, organic synthesis, and electrochemical techniques to present a detailed and study of the adhesion and release of cells and biomolecules to self-assembled systems.

In order to *attach* ligands to the SAM, which in certain cases may promote the interactions of cells or proteins with the surface, they have immobilized ligands at the surface of the SAM via Diels-Alder chemistry. They have created binary component SAMs, with one adsorbate possessing terminal hydroquinone groups that can be reversibly oxidized to quinones, and the diluent adsorbate possessing an oligo(ethy-

lene glycol) group (EG$_3$OH) that resists adventitious sticking of biomolecules. Once oxidized, these pendant, dienophilic quinones then react with incident dienes that can be functionalized with any moiety towards which a cell, protein, or molecule has an affinity. They have, in a simple case, attached a biotin group to a cyclopentadiene moiety, and have demonstrated its covalent coupling to the monolayer by monitoring the levels of streptavidin attachment through surface plasmon resonance spectroscopy [147]. They have also synthesized SAMs that can present a tripeptide recognition factor (arginine–glycine–asparagine, RGD) that has been demonstrated to regulate adhesion in between cells and the extracellular matrices to which they attach. The RGD molecule has been similarly covalently linked to cyclopentadiene, which attaches to the oxidized quinone group. They have monitored the attachment of fibronectin and subsequent attachment of cells to the substrate [146].

An attractive feature of this system is that it is reversible. Once ligands, biomolecules, or cells have been attached to the film, they can be removed by the reduction of that same quinone via an applied potential from the gold substrate (electrode) upon which the SAM is adsorbed. Upon reduction of the quinone moiety, it cyclizes to form a lactone and liberates the attached ligand, eliminating the recognition factor that would signal the proteins or cells to adhere to the surface (biotin–streptavidin, RGD, etc.) [65,285]. Therefore, the adhesion of cells to surfaces can be modulated through control of the electrochemical potentials.

More simply, Mrksich and coworkers have used microcontact printing as a technique to pattern substrates on a larger scale. For example, they have placed methyl-terminated alkanethiol on a gold substrate via a polymer stamp and then have backfilled the bare regions with EG$_3$OH-terminated thiol. They have shown that large biomolecules and cells stick exclusively to the methyl-terminated regions, Fig. 33 [286]. In an elegant combination of using both microcontact printing and electrochemistry, Mrksich and coworkers have demonstrated cell spreading and migration of cells by printing alkanethiol and backfilling with a mixture of EG$_3$OH- and hydroquinone-terminated thiols. Upon oxidation of the hydroquinone and its subsequent reaction with an RGD-ligand, they showed that the cells would migrate from the methyl-terminated regions to those regions presenting recognition factor [147]; in similar experiments, they have demonstrated that a second cell type could be adsorbed in these RGD-presenting ligands before spreading of the cell type that was adsorbed to the methyl-terminated region by a fibronectin adhesion layer [287].

9.1.1. Microcontact printing of proteins and other biomolecules

Biomolecules have been placed on substrates through μCP. Researchers at IBM-Zurich have demonstrated that a protein solution can be directly inked to a PDMS stamp, and a monolayer of protein transfers to the substrate beneath [195,288]. It was demonstrated that some proteins retained their activity upon transfer to a solid substrate. However, for more delicate proteins, it might be possible to functionalize them with biotin handles and then transfer them to a avidin-coated substrate, specifically using self-assembly chemistries as opposed to the generic placement of molecules.
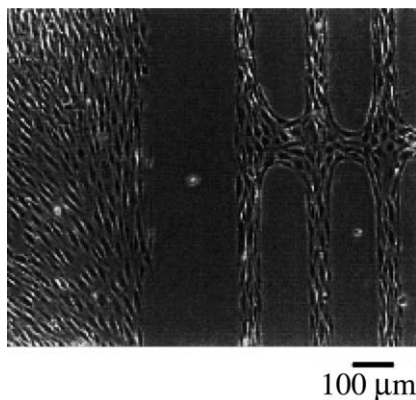
100 μm

Fig. 33. Optical micrograph image of cells patterned on a microcontact-printed, binary component SAM. The SAM was printed with *n*-alkanethiol and backfilled with EG₃OH-terminated alkanethiol. The cells selectively adhere to the methyl-terminated regions. Adapted from Ref. [286], and reproduced with permission of Elsevier Science.

Proteins have also been printed on gold substrates for use in surface plasmon resonance (SPR) assays [289]. The point of this work was to print both wildtype bovine serum albumin (BSA) and then BSA that was functionalized to have an antibody for 2,4-dinitrophenol (2,4-DNP), followed by exposure of the SAM to 2,4-DNP. The bulk refractive index change in the system due to BSA adsorbing to the gold surface was present in both systems, and thus the 2,4-DNP binding event could be isolated by subtracting the background "reference" signal.

9.1.2. Immobilization of enzymes on patterned SAMs

To create functional SAMs, redox-active enzymes have been immobilized on patterned SAMs. One such example is the immobilization of cytochrome *c* on a binary component SAM of 3-mercaptopropionic acid and *n*-hexadecanethiol [290]. Proteins generally adsorb to polar regions through electrostatic interactions, and here the cytochrome *c* molecules adsorb on the 3-MPA regions; higher fractional surface coverage of the 3-MPA corresponds to a greater fractional surface coverage of the cytochrome *c* proteins.

Arnold et al. have also immobilized cytochrome *c* on binary component, phase separated SAMs, with mixtures of *n*-decanethiolate and 11-mercaptoundecanoic acid (while of differing termini, the molecules are approximately the same length) [291]. Reductive desorption of the molecules indicated that the adsorbates were mixed on the local scale, as separate peaks for the desorption of the individual components could not be detected. They report that the desorption potential shifts linearly with the mole fractions of the adsorbates (as compared to the individual reduction potentials of each molecule), and thus they propose that the relative surface coverages of each adsorbate roughly mirrors that of the mole fraction of the adsorbates mixed in solution.

Nelson et al. have investigated the ability of cells to adhere and to spread by printing different types of materials on substrates that are known to be non-adhesive [292], while Capadona et al. examined the effects of fibronectin and cell adhesion on mixed SAMs composed of methyl- and oEG-terminated alkanethiolates [293].

10. Conclusions and prospects

With the techniques of patterning SAMs that are currently available and with those that now being developed, significant advances in the construction, manipulation, and function can be made in a variety of materials. Understanding the underlying processes and mechanisms of surface-based assembly will enable more universal patterning capabilities, reaching down to the nanometer scale. Exploiting the interactions (either favorable or weak) between neighboring molecules has led to self-assembled nanostructures being used as viable biomolecular arrays and scaffolds, lithography resists, molecular nanoelectronic assemblies, and other structures created from the "bottom up". The patterning of self-assembled monolayers and the technologies arising from it, holds promise for enabling the placement of selective functionality at the molecular scale by using and controlling the interactions of the molecules selected.

Acknowledgements

References

[1] L.C. Giancarlo, G.W. Flynn, Ann. Rev. Phys. Chem. 49 (1998) 297.
[2] L.L. Kesmodel, L.H. Dubois, G.A. Somorjai, Chem. Phys. Lett. 56 (1978) 267.
[3] R.G. Nuzzo, D.L. Allara, J. Am. Chem. Soc. 105 (1983) 4481.
[4] R.G. Nuzzo, B.R. Zegarski, L.H. Dubois, J. Am. Chem. Soc. 109 (1987) 733.
[5] J. Sagiv, J. Am. Chem. Soc. 102 (1980) 92.
[6] G.M. Whitesides, B. Grzybowski, Science 295 (2002) 2418.
[7] P. Allongue, C.H. de Villeneuve, J. Pinson, F. Ozanam, J.N. Chazalviel, X. Wallart, Electrochim. Acta 43 (1998) 2791.
[8] J.L. He, Z.H. Lu, S.A. Mitchell, D.D.M. Wayner, J. Am. Chem. Soc. 120 (1998) 2660.
[9] M.-C. Bernard, A. Chaussé, E. Cabet-Deliry, M.M. Chehimi, J. Pinson, F. Podvorica, C. Vautrin-Ul, Chem. Mater. 15 (2003) 3450.
[10] D.V. Kosynkin, J.M. Tour, Org. Lett. 3 (2001) 993.
[11] A. Ulman, Chem. Rev. 96 (1996) 1533.

[12] D.L. Allara, A.N. Parikh, F. Rondelez, Langmuir 11 (1995) 2357.
[13] A.N. Parikh, M.A. Schivley, E. Koo, K. Seshadri, D. Aurentz, K. Mueller, D.L. Allara, J. Am. Chem. Soc. 119 (1997) 3135.
[14] D.L. Allara, R.G. Nuzzo, Langmuir 1 (1985) 45.
[15] P.E. Laibinis, J.J. Hickman, M.S. Wrighton, G.M. Whitesides, Science 245 (1989) 845.
[16] P.E. Laibinis, G.M. Whitesides, J. Am. Chem. Soc. 114 (1992) 1990.
[17] C.D. Bain, E.B. Troughton, Y.T. Tao, J. Evall, G.M. Whitesides, R.G. Nuzzo, J. Am. Chem. Soc. 111 (1989) 321.
[18] P.E. Laibinis, M.A. Fox, J.P. Folkers, G.M. Whitesides, Langmuir 7 (1991) 3167.
[19] J. Chen, M.A. Reed, A.M. Rawlett, J.M. Tour, Science 286 (1999) 1550.
[20] J. Chen, L.C. Calvet, M.A. Reed, D.W. Carr, D.S. Grubisha, D.W. Bennett, Chem. Phys. Lett. 313 (1999) 741.
[21] L.A. Bumm, J.J. Arnold, T.D. Dunbar, D.L. Allara, P.S. Weiss, J. Phys. Chem. B 103 (1999) 8122.
[22] M.D. Porter, T.B. Bright, D.L. Allara, C.E.D. Chidsey, J. Am. Chem. Soc. 109 (1987) 3559.
[23] C.E.D. Chidsey, C.R. Bertozzi, T.M. Putvinski, A.M. Mujsce, J. Am. Chem. Soc. 112 (1990) 4301.
[24] S.B. Sachs, S.P. Dudek, R.P. Hsung, L.R. Sita, J.F. Smalley, M.D. Newton, S.W. Feldberg, C.E.D. Chidsey, J. Am. Chem. Soc. 119 (1997) 10563.
[25] H.D. Sikes, J.F. Smalley, S.P. Dudek, A.R. Cook, M.D. Newton, C.E.D. Chidsey, S.W. Feldberg, Science 291 (2001) 1519.
[26] A.A. Dhirani, R.W. Zehner, R.P. Hsung, P. Guyot-Sionnest, L.R. Sita, J. Am. Chem. Soc. 118 (1996) 3319.
[27] T. Ishida, W. Mizutani, H. Azehara, F. Sato, N. Choi, U. Akiba, M. Fujihira, H. Tokumoto, Langmuir 17 (2001) 7459.
[28] T. Ishida, W. Mizutani, N. Choi, U. Akiba, M. Fujihira, H. Tokumoto, J. Phys. Chem. B 104 (2000) 11680.
[29] G.H. Yang, Y.L. Qian, C. Engtrakul, L.R. Sita, G.-Y. Liu, J. Phys. Chem. B 104 (2000) 9059.
[30] D.N. Batchelder, S.D. Evans, T.L. Freeman, L. Häussling, H. Ringsdorf, H. Wolf, J. Am. Chem. Soc. 116 (1994) 1050.
[31] T. Kim, Q. Ye, L. Sun, K.C. Chan, R.M. Crooks, Langmuir 12 (1996) 6065.
[32] V. Chechik, R.M. Crooks, C.J.M. Stirling, Adv. Mater. 12 (2000) 1161.
[33] M.D. Mowery, A.C. Smith, C.E. Evans, Langmuir 16 (2000) 5998.
[34] R.S. Clegg, J.E. Hutchison, Langmuir 12 (1996) 5239.
[35] R.S. Clegg, S.M. Reed, R.K. Smith, B.L. Barron, J.A. Rear, J.E. Hutchison, Langmuir 15 (1999) 8876.
[36] S.-W. Tam-Chang, H. Biebuyck, G.M. Whitesides, N. Jeon, R.G. Nuzzo, Langmuir 11 (1995) 4371.
[37] A.J. Pertsin, M. Grunze, H.J. Kreuzer, R.L.C. Wang, Phys. Chem. Chem. Phys. (2000) 1729.
[38] R.L.C. Wang, H.J. Kreuzer, M. Grunze, J. Phys. Chem. B 101 (1997) 9767.
[39] R.L.C. Wang, H.J. Kreuzer, M. Grunze, A.J. Pertsin, Phys. Chem. Chem. Phys. (2000) 1721.
[40] C.D. Bain, G.M. Whitesides, J. Am. Chem. Soc. 110 (1988) 6560.
[41] C.D. Bain, H.A. Biebuyck, G.M. Whitesides, Langmuir 5 (1989) 723.
[42] G.-Y. Liu, P. Fenter, C.E.D. Chidsey, D.F. Ogletree, P. Eisenberger, M. Salmeron, J. Chem. Phys. 101 (1994) 4301.
[43] E.M. Cheadle, D.N. Batchelder, S.D. Evans, H.L. Zhang, H. Fukushima, S. Miyashita, M. Graupe, A. Puck, O.E. Shmakova, R. Colorado, T.R. Lee, Langmuir 17 (2001) 6616.
[44] C.D. Bain, G.M. Whitesides, J. Am. Chem. Soc. 110 (1988) 3665.
[45] C.D. Bain, G.M. Whitesides, J. Am. Chem. Soc. 111 (1989) 7164.
[46] H.A. Biebuyck, C.D. Bain, G.M. Whitesides, Langmuir 10 (1994) 1825.
[47] C.D. Bain, G.M. Whitesides, J. Am. Chem. Soc. 110 (1988) 5897.
[48] M. Sprik, E. Delamarche, B. Michel, U. Röthlisberger, M.L. Klein, H. Wolf, H. Ringsdorf, Langmuir 10 (1994) 4116.
[49] J. Cheng, G. Sàghi-Szabó, J.A. Tossell, C.J. Miller, J. Am. Chem. Soc. 118 (1996) 680.
[50] C.D. Bain, G.M. Whitesides, Langmuir 5 (1989) 1370.
[51] C.D. Bain, J. Evall, G.M. Whitesides, J. Am. Chem. Soc. 111 (1989) 7155.

[52] A. Hooper, G.L. Fisher, K. Konstadinidis, D. Jung, H. Nguyen, R. Opila, R.W. Collins, N. Winograd, D.L. Allara, J. Am. Chem. Soc. 121 (1999) 8052.
[53] R.S. Clegg, J.E. Hutchison, J. Am. Chem. Soc. 121 (1999) 5319.
[54] D.W. Mosley, M.A. Sellmeyer, E.J. Daida, J.M. Jacobson, J. Am. Chem. Soc. 125 (2003) 10532.
[55] S. Frey, A. Shaporenko, M. Zharnikov, P. Harder, D.L. Allara, J. Phys. Chem. B 107 (2003) 7716.
[56] J. Tien, A. Terfort, G.M. Whitesides, Langmuir 13 (1997) 5349.
[57] R.I. Carey, J.P. Folkers, G.M. Whitesides, Langmuir 10 (1994) 2228.
[58] H. Menzel, M.D. Mowery, M. Cai, C.E. Evans, J. Phys. Chem. B 102 (1998) 9550.
[59] D.L. Dermody, Y.S. Lee, T. Kim, R.M. Crooks, Langmuir 15 (1999) 8435.
[60] F. Buckel, F. Effenberger, C. Yan, A. Gölzhäuser, M. Grunze, Adv. Mater. 12 (2000) 901.
[61] J.M. Tour, L. Jones II II, D.L. Pearson, J.J.S. Lamba, T.P. Burgin, G.M. Whitesides, D.L. Allara, A.N. Parikh, S.V. Atre, J. Am. Chem. Soc. 117 (1995) 9529.
[62] L.A. Bumm, J.J. Arnold, M.T. Cygan, T.D. Dunbar, T.P. Burgin, L. Jones II, D.L. Allara, J.M. Tour, P.S. Weiss, Science 271 (1996) 1705.
[63] Z.J. Donhauser, B.A. Mantooth, K.F. Kelly, L.A. Bumm, J.D. Monnell, J.J. Stapleton, D.W. Price Jr., A.M. Rawlett, D.L. Allara, J.M. Tour, P.S. Weiss, Science 292 (2001) 2303.
[64] A.A. Dhirani, P.H. Lin, P. Guyot-Sionnest, R.W. Zehner, L.R. Sita, J. Chem. Phys. 106 (1997) 5249.
[65] C.D. Hodneland, M. Mrksich, J. Am. Chem. Soc. 122 (2000) 4235.
[66] K.L. Prime, G.M. Whitesides, J. Am. Chem. Soc. 115 (1993) 10714.
[67] G.B. Sigal, C. Bamdad, A. Barberis, J. Strominger, G.M. Whitesides, Anal. Chem. 68 (1996) 490.
[68] C. Roberts, C.S. Chen, M. Mrksich, V. Martichonok, D.E. Ingber, G.M. Whitesides, J. Am. Chem. Soc. 120 (1998) 6548.
[69] S.D. Evans, K.E. Goppert-Berarducci, E. Urankar, L.J. Gerenser, A. Ulman, Langmuir 7 (1991) 2700.
[70] L.J. Yeager, D.G. Amirsakis, E. Newman, R.L. Garrell, Tetrahedron Lett. 39 (1998) 8409.
[71] B.I. Ipe, K.G. Thomas, S. Barazzouk, S. Hotchandani, P.V. Kamat, J. Phys. Chem. B 106 (2002) 18.
[72] F. Nakamura, M. Hara, Mol. Cryst. Liquid Cryst. 377 (2002) 57.
[73] H. Wolf, H. Ringsdorf, E. Delamarche, T. Takami, H. Kang, B. Michel, C. Gerber, M. Jaschke, H.J. Butt, E. Bamberg, J. Phys. Chem. 99 (1995) 7102.
[74] T. Takami, E. Delamarche, B. Michel, C. Gerber, H. Wolf, H. Ringsdorf, Langmuir 11 (1995) 3876.
[75] L.O. Brown, J.E. Hutchison, J. Am. Chem. Soc. 121 (1999) 882.
[76] L.O. Brown, J.E. Hutchison, J. Phys. Chem. B 105 (2001) 8911.
[77] D.V. Leff, L. Brandt, J.R. Heath, Langmuir 12 (1996) 4723.
[78] M.G. Samant, C.A. Brown, J.G. Gordon, Langmuir 8 (1992) 1615.
[79] E.L. Smith, M.D. Porter, J. Phys. Chem. 97 (1993) 8032.
[80] J.I. Henderson, S. Feng, G.M. Ferrence, T. Bein, C.P. Kubiak, Inorg. Chim. Acta 242 (1996) 115.
[81] J.J. Hickman, C.F. Zou, D. Ofer, P.D. Harvey, M.S. Wrighton, P.E. Laibinis, C.D. Bain, G.M. Whitesides, J. Am. Chem. Soc. 111 (1989) 7271.
[82] K. Shimazu, Y. Sato, I. Yagi, K. Uosaki, Bull. Chem. Soc. Jpn. 67 (1994) 863.
[83] H. Sellers, Surf. Sci. 264 (1992) 177.
[84] P.E. Laibinis, G.M. Whitesides, J. Am. Chem. Soc. 114 (1992) 9022.
[85] K. Slowinski, R.V. Chamberlain, C.J. Miller, M. Majda, J. Am. Chem. Soc. 119 (1997) 11910.
[86] M.J. Lercel, R.C. Tiberio, P.F. Chapman, H.G. Craighead, C.W. Sheen, A.N. Parikh, D.L. Allara, J. Vac. Sci. Technol. B 11 (1993) 2823.
[87] O.S. Nakagawa, S. Ashok, C.W. Sheen, J. Martensson, D.L. Allara, Jpn. J. Appl. Phys. 30 (1991) 3759.
[88] H. Yamamoto, R.A. Butera, Y. Gu, D.H. Waldeck, Langmuir 15 (1999) 8640.
[89] M.A. Marcus, W. Flood, M. Stiegerwald, L. Brus, M. Bawendi, J. Phys. Chem. 95 (1991) 1572.
[90] J. Gun, J. Sagiv, J. Coll. Interf. Sci. 112 (1986) 457.
[91] U. Diebold, Surf. Sci. Rep. 48 (2003) 53.
[92] X. Marguerettaz, D. Fitzmaurice, Langmuir 13 (1997) 6769.
[93] J.E. Ritchie, C.A. Wells, J.P. Zhou, J.N. Zhao, J.T. McDevitt, C.R. Ankrum, L. Jean, D.R. Kanis, J. Am. Chem. Soc. 120 (1998) 2733.

[94] F. Xu, K.M. Chen, R.D. Piner, C.A. Mirkin, J.E. Ritchie, J.T. McDevitt, Langmuir 14 (1998) 6505.
[95] K.M. Chen, F. Xu, C.A. Mirkin, R.K. Lo, K.S. Nanjundaswamy, J.P. Zhou, J.T. McDevitt, Langmuir 12 (1996) 2622.
[96] R.A. Hatton, S.R. Day, M.A. Chesters, M.R. Willis, Thin Solid Films 394 (2001) 292.
[97] C. Yan, M. Zharnikov, A. Gölzhäuser, M. Grunze, Langmuir 16 (2000) 6208.
[98] A. Kumar, G.M. Whitesides, Appl. Phys. Lett. 63 (1993) 2002.
[99] J.L. Wilbur, A. Kumar, E. Kim, G.M. Whitesides, Adv. Mater. 6 (1994) 600.
[100] E. Kim, A. Kumar, G.M. Whitesides, J. Electrochem. Soc. 142 (1995) 628.
[101] C.B. Gorman, H.A. Biebuyck, G.M. Whitesides, Chem. Mater. 7 (1995) 252.
[102] Y.N. Xia, X.M. Zhao, G.M. Whitesides, Microelectron. Eng. 32 (1996) 255.
[103] E. Delamarche, A.C.F. Hoole, B. Michel, S. Wilkes, M. Despont, M.E. Welland, H. Biebuyck, J. Phys. Chem. B 101 (1997) 9263.
[104] M. Geissler, H. Schmid, A. Bietsch, B. Michel, E. Delamarche, Langmuir 18 (2002) 2374.
[105] J.C. Love, D.B. Wolfe, M.L. Chabinyc, K.E. Paul, G.M. Whitesides, J. Am. Chem. Soc. 124 (2002) 1576.
[106] R.J. Jackman, J.L. Wilbur, G.M. Whitesides, Science 269 (1995) 664.
[107] G.P. López, M.W. Albers, S.L. Schreiber, R. Carroll, E. Peralta, G.M. Whitesides, J. Am. Chem. Soc. 115 (1993) 5877.
[108] R.G. Nuzzo, L.H. Dubois, D.L. Allara, J. Am. Chem. Soc. 112 (1990) 558.
[109] G.E. Poirier, E.D. Pylant, Science 272 (1996) 1145.
[110] L.H. Dubois, R.G. Nuzzo, Ann. Rev. Phys. Chem. 43 (1992) 437.
[111] P.E. Laibinis, G.M. Whitesides, D.L. Allara, Y.T. Tao, A.N. Parikh, R.G. Nuzzo, J. Am. Chem. Soc. 113 (1991) 7152.
[112] Z.J. Donhauser, D.W. Price II, J.M. Tour, P.S. Weiss, J. Am. Chem. Soc. 125 (2003) 11462.
[113] C.E.D. Chidsey, Science 251 (1991) 919.
[114] T.W. Schneider, D.A. Buttry, J. Am. Chem. Soc. 115 (1993) 12391.
[115] D.S. Karpovich, G.J. Blanchard, Langmuir 10 (1994) 3315.
[116] H.M. Schessler, D.S. Karpovich, G.J. Blanchard, J. Am. Chem. Soc. 118 (1996) 9645.
[117] N. Camillone III, P. Eisenberger, T.Y.B. Leung, P. Schwartz, G. Scoles, G.E. Poirier, M.J. Tarlov, J. Chem. Phys. 101 (1994) 11031.
[118] D. Anselmetti, A. Baratoff, H.-J. Güntherodt, E. Delamarche, B. Michel, C. Gerber, H. Kang, H. Wolf, H. Ringsdorf, Europhys. Lett. 27 (1994) 365.
[119] E. Delamarche, B. Michel, C. Gerber, D. Anselmetti, H.-J. Güntherodt, H. Wolf, H. Ringsdorf, Langmuir 10 (1994) 2869.
[120] S.J. Stranick, A.N. Parikh, Y.T. Tao, D.L. Allara, P.S. Weiss, J. Phys. Chem. 98 (1994) 7636.
[121] G.E. Poirier, Chem. Rev. 97 (1997) 1117.
[122] U. Dürig, O. Zuger, B. Michel, L. Häussling, H. Ringsdorf, Phys. Rev. B 48 (1993) 1711.
[123] R.D. Piner, J. Zhu, F. Xu, S.H. Hong, C.A. Mirkin, Science 283 (1999) 661.
[124] G.-Y. Liu, S. Xu, Y.L. Qian, Acc. Chem. Res. 33 (2000) 457.
[125] K. Edinger, M. Grunze, C. Wöll, Phys. Chem. Chem. Phys. 101 (1997) 1811.
[126] G.E. Poirier, Langmuir 13 (1997) 2019.
[127] G. Yang, G.-Y. Liu, J. Phys. Chem. B 107 (2003) 8746.
[128] G.E. Poirier, M.J. Tarlov, Langmuir 10 (1994) 2853.
[129] S.J. Stranick, A.N. Parikh, D.L. Allara, P.S. Weiss, J. Phys. Chem. (1994) 11136.
[130] L.A. Bumm, J.J. Arnold, L.F. Charles, T.D. Dunbar, D.L. Allara, P.S. Weiss, J. Am. Chem. Soc. 121 (1999) 8017.
[131] M.T. Cygan, T.D. Dunbar, J.J. Arnold, L.A. Bumm, N.F. Shedlock, T.P. Burgin, L. Jones, D.L. Allara, J.M. Tour, P.S. Weiss, J. Am. Chem. Soc. (1998) 2721.
[132] J.B. Schlenoff, M. Li, H. Ly, J. Am. Chem. Soc. 117 (1995) 12528.
[133] A. Carvalho, M. Geissler, H. Schmid, B. Michel, E. Delamarche, Langmuir 18 (2002) 2406.
[134] Y. Xia, E. Kim, G.M. Whitesides, J. Electrochem. Soc. 143 (1996) 1070.
[135] Y.N. Xia, E. Kim, M. Mrksich, G.M. Whitesides, Chem. Mater. 8 (1996) 601.
[136] A.B.D. Cassie, Discuss. Faraday Soc. 3 (1948) 11.

[137] E.B. Troughton, C.D. Bain, G.M. Whitesides, R.G. Nuzzo, D.L. Allara, M.D. Porter, Langmuir 4 (1988) 365.
[138] P.E. Laibinis, R.G. Nuzzo, G.M. Whitesides, J. Phys. Chem. 96 (1992) 5097.
[139] D.L. Allara, R.G. Nuzzo, Langmuir 1 (1985) 52.
[140] M.A. Bryant, J.E. Pemberton, J. Am. Chem. Soc. (1991) 3629.
[141] M.A. Bryant, J.E. Pemberton, J. Am. Chem. Soc. (1991) 8284.
[142] H.O. Finklea, S. Avery, M. Lynch, T. Furtsch, Langmuir 3 (1987) 409.
[143] E. Sabatani, I. Rubinstein, J. Phys. Chem. 91 (1987) 6663.
[144] E. Sabatani, I. Rubinstein, R. Maoz, J. Sagiv, J. Electroanal. Chem. 219 (1987) 365.
[145] H.O. Finklea, D.A. Snider, J. Fedyk, Langmuir 6 (1990) 371.
[146] M.N. Yousaf, B.T. Houseman, M. Mrksich, Angew. Chem., Int. Ed. 40 (2001) 1093.
[147] M.N. Yousaf, M. Mrksich, J. Am. Chem. Soc. 121 (1999) 4286.
[148] W. Mizutani, Jpn. J. Appl. Phys. 38 (1999) 7260.
[149] S.-I. Imabayashi, D. Hobara, T. Kakiuchi, Langmuir 13 (1997) 4502.
[150] V.M. Mirsky, Trends Anal. Chem. 21 (2002) 439.
[151] C.J. Chen, Introduction to Scanning Tunneling Microscopy, Oxford Series in Optical and Imaging Sciences, Oxford University Press, New York, 1993.
[152] D.A. Bonnell, Scanning Probe Microscopy and Spectroscopy: Theory, Techniques, and Applications, second ed., Wiley–VCH, Inc., New York, 2001.
[153] G. Binnig, H. Rohrer, IBM J. Res. Devel. 30 (1986) 355.
[154] P. Sautet, Chem. Rev. 97 (1997) 1097.
[155] G. Binnig, C.F. Quate, C. Gerber, Phys. Rev. Lett. 56 (1986) 930.
[156] G. Binnig, C. Gerber, E. Stoll, T.R. Albrecht, C.F. Quate, Surf. Sci. 189 (1987) 1.
[157] G. Binnig, C. Gerber, E. Stoll, T.R. Albrecht, C.F. Quate, Europhys. Lett. 3 (1987) 1281.
[158] J.L. Wilbur, H.A. Biebuyck, J.C. Macdonald, G.M. Whitesides, Langmuir 11 (1995) 825.
[159] J.A. Zasadzinski, Curr. Opin. Coll. Interf. Sci. 1 (1996) 264.
[160] R. Wiesendanger, Curr. Opin. Solid State Mater. Sci. 4 (1999) 435.
[161] H.J. Hug, A. Moser, T. Jung, O. Fritz, A. Wadas, I. Parashikov, H.-J. Güntherodt, Rev. Sci. Instrum. 64 (1993) 2920.
[162] A. Gruverman, O. Auciello, H. Tokumoto, Integr. Ferroelectr. 19 (1998) 49.
[163] M. Fujihira, Ann. Rev. Mater. Sci. 29 (1999) 353.
[164] H. Bluhm, A. Wadas, R. Wiesendanger, K.P. Meyer, L. Szczesniak, Phys. Rev. B 55 (1997) 4.
[165] Y. Suguwara, T. Uchihashi, M. Abe, S. Morita, Appl. Surf. Sci. 140 (1999) 371.
[166] A. Born, R. Wiesendanger, Appl. Phys. A 66 (1998) 421.
[167] S. Lanyi, J. Torok, P. Rehurek, J. Vac. Sci. Technol. B 14 (1996) 892.
[168] A. Noy, D.V. Vezenov, C.M. Lieber, Ann. Rev. Mater. Sci. 27 (1997) 381.
[169] A. Noy, C.D. Frisbie, L.F. Rozsnyai, M.S. Wrighton, C.M. Lieber, J. Am. Chem. Soc. 117 (1995) 7943.
[170] J.P. Folkers, P.E. Laibinis, G.M. Whitesides, Langmuir 8 (1992) 1330.
[171] D. Hobara, T. Sasaki, S. Imabayashi, T. Kakiuchi, Langmuir 15 (1999) 5073.
[172] R.K. Smith, S.M. Reed, P.A. Lewis, J.D. Monnell, R.S. Clegg, K.F. Kelly, L.A. Bumm, J.E. Hutchison, P.S. Weiss, J. Phys. Chem. B 105 (2001) 1119.
[173] P.A. Lewis, R.K. Smith, K.F. Kelly, L.A. Bumm, S.M. Reed, R.S. Clegg, J.D. Gunderson, J.E. Hutchison, P.S. Weiss, J. Phys. Chem. B 105 (2001) 10630.
[174] J.P. Folkers, P.E. Laibinis, G.M. Whitesides, J. Adhes. Sci. Technol. 6 (1992) 1397.
[175] J.P. Folkers, P.E. Laibinis, G.M. Whitesides, J. Deutch, J. Phys. Chem. 98 (1994) 563.
[176] D. Hobara, T. Kakiuchi, Electrochem. Commun. 3 (2001) 154.
[177] T. Kakiuchi, M. Iida, N. Gon, D. Hobara, S. Imabayashi, K. Niki, Langmuir 17 (2001) 1599.
[178] T. Sawaguchi, Y. Sato, F. Mizutani, J. Electroanal. Chem. 496 (2001) 50.
[179] V.M. Mirsky, T. Hirsch, S.A. Piletsky, O.S. Wolfbeis, Angew. Chem., Int. Ed. 38 (1999) 1108.
[180] S.A. Piletsky, E.V. Piletskaya, T.A. Sergeyeva, T.L. Panasyuk, A.V. El'skaya, Sens. Actuator B 60 (1999) 216.

[181] M.E. Anderson, R.K. Smith, Z.J. Donhauser, A. Hatzor, P.A. Lewis, L.P. Tan, H. Tanaka, M.W. Horn, P.S. Weiss, J. Vac. Sci. Technol. B 20 (2002) 2739.

[182] Z.J. Donhauser, B.A. Mantooth, T.P. Pearl, K.F. Kelly, S.U. Nanayakkara, P.S. Weiss, Jpn. J. Appl. Phys. 41 (2002) 4871.

[183] C.A. Widrig, C. Chung, M.D. Porter, J. Electroanal. Chem. 310 (1991) 335.

[184] C.J. Zhong, M.D. Porter, J. Electroanal. Chem. 425 (1997) 147.

[185] H. Wano, K. Uosaki, Langmuir 17 (2001) 8224.

[186] M.J. Esplandiu, H. Hagenstrom, D.M. Kolb, Langmuir 17 (2001) 828.

[187] T. Hirsch, H. Kettenberger, O.S. Wolfbeis, V.M. Mirsky, Chem. Commun. 3 (2003) 432.

[188] H. Munakata, S. Kuwabata, Y. Ohko, H. Yoneyama, J. Electroanal. Chem. 496 (2001) 29.

[189] T. Kakiuchi, K. Sato, M. Iida, D. Hobara, S. Imabayashi, K. Niki, Langmuir 16 (2000) 7238.

[190] S.-I. Imabayashi, D. Hobara, T. Kakiuchi, Langmuir 17 (2001) 2560.

[191] M. Satjapipat, R. Sanedrin, F.M. Zhou, Langmuir 17 (2001) 7637.

[192] T. Wilhelm, G. Wittstock, Electrochim. Acta 47 (2001) 275.

[193] Y.N. Xia, G.M. Whitesides, Angew. Chem., Int. Ed. 37 (1998) 551.

[194] A. Kumar, H.A. Biebuyck, G.M. Whitesides, Langmuir 10 (1994) 1498.

[195] B. Michel, A. Bernard, A. Bietsch, E. Delamarche, M. Geissler, D. Juncker, H. Kind, J.P. Renault, H. Rothuizen, H. Schmid, P. Schmidt-Winkel, R. Stutz, H. Wolf, IBM J. Res. Devel. 45 (2001) 697.

[196] X.M. Zhao, Y.N. Xia, G.M. Whitesides, J. Mater. Chem. 7 (1997) 1069.

[197] T.W. Odom, V.R. Thalladi, J.C. Love, G.M. Whitesides, J. Am. Chem. Soc. (2002) 12112.

[198] Y.N. Xia, J. Tien, D. Qin, G.M. Whitesides, Langmuir 12 (1996) 4033.

[199] A. Bietsch, B. Michel, J. Appl. Phys. 88 (2000) 4310.

[200] H. Schmid, B. Michel, Macromolecules 33 (2000) 3042.

[201] G. Bar, S. Rubin, A.N. Parikh, B.I. Swanson, T.A. Zawodzinski, M.H. Whangbo, Langmuir 13 (1997) 373.

[202] D. Fischer, A. Marti, G. Hahner, J. Vac. Sci. Technol. A 15 (1997) 2173.

[203] N.B. Larsen, H. Biebuyck, E. Delamarche, B. Michel, J. Am. Chem. Soc. 119 (1997) 3017.

[204] N.L. Jeon, K. Finnie, K. Branshaw, R.G. Nuzzo, Langmuir 13 (1997) 3382.

[205] E. Delamarche, H. Schmid, A. Bietsch, N.B. Larsen, H. Rothuizen, B. Michel, H. Biebuyck, J. Phys. Chem. B 102 (1998) 3324.

[206] L. Libioulle, A. Bietsch, H. Schmid, B. Michel, E. Delamarche, Langmuir 15 (1999) 300.

[207] A.S. Eberhardt, R.M. Nyquist, A.N. Parikh, T. Zawodzinski, B.I. Swanson, Langmuir 15 (1999) 1595.

[208] D.J. Graham, D.D. Price, B.D. Ratner, Langmuir 18 (2002) 1518.

[209] L. Yan, C. Marzolin, A. Terfort, G.M. Whitesides, Langmuir 13 (1997) 6704.

[210] L. Yan, X.M. Zhao, G.M. Whitesides, J. Am. Chem. Soc. 120 (1998) 6179.

[211] J. Lahiri, E. Ostuni, G.M. Whitesides, Langmuir 15 (1999) 2055.

[212] P.T. Hammond, G.M. Whitesides, Macromolecules 28 (1995) 7569.

[213] S.L. Clark, P.T. Hammond, Adv. Mater. 10 (1998) 1515.

[214] K.M. Chen, X.P. Jiang, L.C. Kimerling, P.T. Hammond, Langmuir 16 (2000) 7825.

[215] I. Lee, H.P. Zheng, M.F. Rubner, P.T. Hammond, Adv. Mater. 14 (2002) 572.

[216] H.P. Zheng, I. Lee, M.F. Rubner, P.T. Hammond, Adv. Mater. 14 (2002) 569.

[217] J. Aizenberg, A.J. Black, G.M. Whitesides, J. Am. Chem. Soc. 121 (1999) 4500.

[218] J. Aizenberg, A.J. Black, G.M. Whitesides, Nature 398 (1999) 495.

[219] J. Aizenberg, A.J. Black, G.M. Whitesides, Nature 394 (1998) 868.

[220] S.W. Han, I. Lee, K. Kim, Langmuir 18 (2002) 182.

[221] S.L. Clark, E.S. Handy, M.F. Rubner, P.T. Hammond, Adv. Mater. 11 (1999) 1031.

[222] S.L. Clark, P.T. Hammond, Langmuir 16 (2000) 10206.

[223] A. Kumar, H.A. Biebuyck, N.L. Abbott, G.M. Whitesides, J. Am. Chem. Soc. 114 (1992) 9188.

[224] A. Kumar, N.L. Abbott, E. Kim, H.A. Biebuyck, G.M. Whitesides, Acc. Chem. Res. 28 (1995) 219.

[225] A.J. Black, K.E. Paul, J. Aizenberg, G.M. Whitesides, J. Am. Chem. Soc. 121 (1999) 8356.

[226] E. Kim, G.M. Whitesides, M.B. Freiler, M. Levy, J.L. Lin, R.M. Osgood, Nanotechnology 7 (1996) 266.

[227] Y.-L. Loo, R.L. Willett, K.W. Baldwin, J.A. Rogers, J. Am. Chem. Soc. 124 (2002) 7654.
[228] A. Hatzor, P.S. Weiss, Science 291 (2001) 1019.
[229] W.J. Dressick, J.M. Calvert, Jpn. J. Appl. Phys. 32 (1993) 5829.
[230] J.M. Calvert, J. Vac. Sci. Technol. B 11 (1993) 2155.
[231] C.S. Whelan, M.J. Lercel, H.G. Craighead, K. Seshadri, D.L. Allara, Appl. Phys. Lett. 69 (1996) 4245.
[232] R.C. Tiberio, H.G. Craighead, M. Lercel, T. Lau, C.W. Sheen, D.L. Allara, Appl. Phys. Lett. 62 (1993) 476.
[233] D.W. Carr, M.J. Lercel, C.S. Whelan, H.G. Craighead, K. Seshadri, D.L. Allara, J. Vac. Sci. Technol. A 15 (1997) 1446.
[234] W. Eck, V. Stadler, W. Geyer, M. Zharnikov, A. Gölzhäuser, M. Grunze, Adv. Mater. 12 (2000) 805.
[235] W. Geyer, V. Stadler, W. Eck, M. Zharnikov, A. Gölzhäuser, M. Grunze, Appl. Phys. Lett. 75 (1999) 2401.
[236] W. Geyer, V. Stadler, W. Eck, A. Gölzhäuser, M. Grunze, M. Sauer, T. Weimann, P. Hinze, J. Vac. Sci. Technol. B 19 (2001) 2732.
[237] A. Gölzhäuser, W. Geyer, V. Stadler, W. Eck, M. Grunze, K. Edinger, T. Weimann, P. Hinze, J. Vac. Sci. Technol. B 18 (2000) 3414.
[238] A. Gölzhäuser, W. Eck, W. Geyer, V. Stadler, T. Weimann, P. Hinze, M. Grunze, Adv. Mater. 13 (2001) 806.
[239] T. Weimann, W. Geyer, P. Hinze, V. Stadler, W. Eck, A. Gölzhäuser, Microelectron. Eng. 57–58 (2001) 903.
[240] M. Zharnikov, S. Frey, K. Heister, M. Grunze, Langmuir 16 (2000) 2697.
[241] M. Zharnikov, W. Geyer, A. Gölzhäuser, S. Frey, M. Grunze, Phys. Chem. Chem. Phys. 1 (1999) 3163.
[242] C.K. Harnett, K.M. Satyalakshmi, H.G. Craighead, Appl. Phys. Lett. 76 (2000) 2466.
[243] C.K. Harnett, K.M. Satyalakshmi, H.G. Craighead, Langmuir 17 (2001) 178.
[244] A. Bard, K.K. Berggren, J.L. Wilbur, J.D. Gillaspy, S.L. Rolston, J.J. McClelland, W.D. Phillips, M. Prentiss, G.M. Whitesides, J. Vac. Sci. Technol. B 15 (1997) 1805.
[245] H. Sugimura, T. Hanji, O. Takai, T. Masuda, H. Misawa, Electrochim. Acta 47 (2001) 103.
[246] R. Krupke, S. Malik, H.B. Weber, O. Hampe, M.M. Kappes, H. von Lohneysen, Nano Lett. 2 (2002) 1161.
[247] S. Hong, J. Zhu, C.A. Mirkin, Science 286 (1999) 523.
[248] S. Hong, C.A. Mirkin, Science 288 (2000) 1808.
[249] H.A. Biebuyck, G.M. Whitesides, Langmuir 10 (1994) 4581.
[250] B.L. Weeks, A. Noy, A.E. Miller, J.J. De Yoreo, Phys. Rev. Lett. 88 (2002) 255505.
[251] D.A. Weinberger, S. Hong, C.A. Mirkin, B.W. Wessels, T.B. Higgins, Adv. Mater. 12 (2000) 1600.
[252] L.M. Demers, D.S. Ginger, S.J. Park, Z. Li, S.W. Chung, C.A. Mirkin, Science 296 (2002) 1836.
[253] L.M. Demers, S.J. Park, T.A. Taton, Z. Li, C.A. Mirkin, Angew. Chem., Int. Ed. 40 (2001) 3071.
[254] L.M. Demers, C.A. Mirkin, Angew. Chem., Int. Ed. 40 (2001) 3069.
[255] M. Su, X.G. Liu, S.Y. Li, V.P. Dravid, C.A. Mirkin, J. Am. Chem. Soc. 124 (2002) 1560.
[256] K.B. Lee, S.J. Park, C.A. Mirkin, J.C. Smith, M. Mrksich, Science 295 (2002) 1702.
[257] J.C. Smith, K.B. Lee, Q. Wang, M.G. Finn, J.E. Johnson, M. Mrksich, C.A. Mirkin, Nano Lett. (2003) 883.
[258] X.G. Liu, L. Fu, S.H. Hong, V.P. Dravid, C.A. Mirkin, Adv. Mater. 14 (2002) 231.
[259] Y. Zhang, K. Salaita, J.-H. Lim, C.A. Mirkin, Nano Lett. 2 (2002) 1389.
[260] C. Blackledge, D.A. Engebretson, J.D. McDonald, Langmuir 16 (2000) 8317.
[261] J.W. Zhao, K. Uosaki, Nano Lett. 2 (2002) 137.
[262] J.W. Zhao, K. Uosaki, Langmuir 17 (2001) 7784.
[263] H. Sugimura, K. Okiguchi, N. Nakagiri, M. Miyashita, J. Vac. Sci. Technol. B 14 (1996) 4140.
[264] H. Sugimura, O. Takai, N. Nakagiri, J. Vac. Sci. Technol. B 17 (1999) 1605.
[265] H. Sugimura, O. Takai, N. Nakagiri, J. Electroanal. Chem. 473 (1999) 230.
[266] H. Sugimura, N. Nakagiri, J. Vac. Sci. Technol. B 15 (1997) 1394.
[267] R. Maoz, S.R. Cohen, J. Sagiv, Adv. Mater. 11 (1999) 55.

[268] R. Maoz, E. Frydman, S.R. Cohen, J. Sagiv, Adv. Mater. 12 (2000) 725.
[269] R. Maoz, E. Frydman, S.R. Cohen, J. Sagiv, Adv. Mater. 12 (2000) 424.
[270] S. Hoeppener, L.F. Chi, H. Fuchs, Nano Lett. 2 (2002) 459.
[271] S. Xu, S. Miller, P.E. Laibinis, G.-Y. Liu, Langmuir 15 (1999) 7244.
[272] J. Chen, M.A. Reed, C.L. Asplund, A.M. Cassell, M.L. Myrick, A.M. Rawlett, J.M. Tour, P.G. Van Patten, Appl. Phys. Lett. 75 (1999) 624.
[273] M.J. Lercel, G.F. Redinbo, F.D. Pardo, M. Rooks, R.C. Tiberio, P. Simpson, H.G. Craighead, C.W. Sheen, A.N. Parikh, D.L. Allara, J. Vac. Sci. Technol. B 12 (1994) 3663.
[274] C.B. Gorman, R.L. Carroll, Y.F. He, F. Tian, R. Fuierer, Langmuir 16 (2000) 6312.
[275] C.B. Gorman, R.L. Carroll, R.R. Fuierer, Langmuir 17 (2001) 6923.
[276] R.R. Fuierer, R.L. Carroll, D.L. Feldheim, C.B. Gorman, Adv. Mater. 14 (2002) 154.
[277] U. Kleineberg, A. Brechling, M. Sundermann, U. Heinzmann, Adv. Funct. Mater. 11 (2001) 208.
[278] S. Cruchon-Dupeyrat, S. Porthun, G.-Y. Liu, Appl. Surf. Sci. 175 (2001) 636.
[279] S. Sun, G.J. Leggett, Nano Lett. 2 (2002) 1223.
[280] D.G. Castner, B.D. Ratner, Surf. Sci. 500 (2002) 28.
[281] M. Tirrell, E. Kokkoli, M. Biesalski, Surf. Sci. 500 (2002) 61.
[282] B. Kasemo, Surf. Sci. 500 (2002) 656.
[283] N.L. Jeon, H. Baskaran, S.K.W. Dertinger, G.M. Whitesides, L. Van de Water, M. Toner, Natl. Biotechnol. 20 (2002) 826.
[284] X. Jiang, R. Ferrigno, M. Mrksich, G.M. Whitesides, J. Am. Chem. Soc. 125 (2003) 2366.
[285] W.S. Yeo, C.D. Hodneland, M. Mrksich, Chem. Bio. Chem. 2 (2001) 590.
[286] M. Mrksich, L.E. Dike, J. Tien, D.E. Ingber, G.M. Whitesides, Exp. Cell Res. 235 (1997) 305.
[287] M.N. Yousaf, B.T. Houseman, M. Mrksich, Proc. Natl. Acad. Sci. USA 98 (2001) 5992.
[288] A. Bernard, J.P. Renault, B. Michel, H.R. Bosshard, E. Delamarche, Adv. Mater. 12 (2000) 1067.
[289] H.B. Lu, J. Homola, C.T. Campbell, G.G. Nenninger, S.S. Yee, B.D. Ratner, Sens. Actuator B 74 (2001) 91.
[290] D. Hobara, S. Imabayashi, T. Kakiuchi, Nano Lett. 2 (2002) 1021.
[291] S. Arnold, Z.Q. Feng, T. Kakiuchi, W. Knoll, K. Niki, J. Electroanal. Chem. 438 (1997) 91.
[292] C.M. Nelson, S. Raghavan, J.L. Tan, C.S. Chen, Langmuir 19 (2002) 1493.
[293] J.R. Capadona, D.M. Collard, A.J. García, Langmuir 19 (2002) 1847.